Vol. 494: 41–63, 2013
doi: 10.3354/meps10530

MARINE ECOLOGY PROGRESS SERIES
Mar Ecol Prog Ser

Published December 4

# Production of mycosporine-like amino acids by phytoplankton under ultraviolet radiation exposure in the Sub-Antarctic Zone south of Tasmania

**Kadija Oubelkheir[1,4,*], Lesley A. Clementson[2], Gerald F. Moore[1,3], Gavin H. Tilstone[1]**

[1]Plymouth Marine Laboratory, Plymouth PL13DH, UK
[2]CSIRO Marine and Atmospheric Research, Hobart, 7001 Tasmania, Australia
[3]Bio-Optika, Gunnislake PL18 9NQ, UK

[4]*Present address:* CSIRO Land and Water, Dutton Park, 4102 Queensland, Australia

ABSTRACT: Phytoplankton production of mycosporine-like amino acids (MAAs) against the damaging effects of ultraviolet (UV) radiation, and the associated changes in absorption properties, were examined across different trophic regions south of Tasmania, from the Polar Frontal Zone (PFZ) to the Sub-Antarctic Zone (SAZ) and in sub-tropical waters. The MAA concentration and particulate absorption coefficient were determined in the 0 to 100 m layer across a latitudinal gradient from 54 to 44 degrees south. These spatial observations were complemented with daily incubation experiments at 3 stations located in the PFZ and in the SAZ southeast and southwest of Tasmania. MAAs were widespread, with a predominance of primary MAAs such as porphyra-334 in the PFZ and secondary MAAs such as palythenic acid in the stratified waters in the north of the SAZ. Under surface irradiance levels during deck incubation experiments, phytoplankton from the PFZ and SAZ produced significant amounts of MAAs under UVB radiations, and a fraction was released into the dissolved fraction (generally <20% of the total MAAs). MAA production rates in the north of the SAZ ranged from 0.0009 to 0.0436 mg $m^{-3}$ $kJ^{-1}$ UVB $m^{-2}$ southwest and southeast of Tasmania, respectively. Changes in MAA distribution are discussed in relation to environmental factors (UV radiation exposure, mixing, nutrients) and shifts in the phytoplankton assemblage composition. The strong variability in MAA distribution and composition across the study region is driven primarily by UV radiation exposure and vertical mixing and secondarily by species-specific responses to UV radiation.

KEY WORDS: Phytoplankton · UV · Mycosporine-like amino acids · Absorption coefficient



## INTRODUCTION

Solar ultraviolet (UV) radiation can reach ecologically relevant depths and thus significantly impact phytoplankton carbon fixation rates and biogeochemical cycles in marine ecosystems (Zepp et al. 2003). UV radiation depth penetration ranges from a few centimetres in turbid coastal waters to 10s of metres in clear blue waters (Piazena et al. 2002, Tedetti & Sempere 2006) and is a function of both wavelength and the concentration and nature of particulate and dissolved matter. Both UVB (290 to 320 nm) and UVA (320 to 400 nm) radiations can inhibit phytoplankton photosynthesis as shown on

*Email: kadija.oubelkheir@csiro.au

natural assemblages and cultures (Villafañe et al. 2003 and references therein). The impact of UV radiation on photosynthesis will depend on the balance between photo-damage, photo-protection and repair processes. In the Southern Ocean, additional UV radiation due to ozone depletion events can lead to a reduction in phytoplankton daily primary production by up to 12% (Smith et al. 1992, Holm-Hansen & Helbling 1993, Neale et al. 1998b). Despite the global reduction in chlorofluorocarbon (CFC) levels, the recovery of the ozone layer above the Southern Ocean is still uncertain for the coming decades, due to various factors including stratospheric cooling linked to global warming (Weatherhead & Andersen 2006). This underlines a strong need for a better understanding of the phytoplankton response to UV radiation.

Phytoplankton have developed various photo-protection strategies against the deleterious effects of UV radiation, including, but not limited to, the production of photo-protectants such as mycosporine-like amino-acids (MAAs) (Bandaranayake 1998, Rastogi et al. 2010, Carreto & Carignan 2011). MAAs act as effective sunscreens against the photo-inhibition of photosynthesis and photo-oxidative stress associated with UV radiation (Carreto & Carignan 2011). They occur in a large range of phytoplankton species and bacteria (Jeffrey et al. 1997, Sinha et al. 2007), and are widely distributed across geographic areas (Carreto & Carignan 2011). More than 20 different MAAs have been identified to date in the marine environment, with absorption maxima between 309 and 360 nm, thus covering a large range of wavelengths in the UV range (Carreto & Carignan 2011). Most studies on MAA abundance and composition in natural marine phytoplankton populations have been conducted in Antarctic waters, due to increases in incident UVB radiation associated with stratospheric ozone depletion (e.g. Karentz et al. 1991, Bracher & Wiencke 2000, Whitehead et al. 2001). Published studies in temperate or tropical areas have either relied on the absorption signature of the MAAs in the UV wavelength range (Morrison & Nelson 2004, Marcoval et al. 2008) or, when based on high performance liquid chromatography (HPLC) analysis, have been mostly limited to coastal and freshwater systems (Whitehead & Vernet 2000, Llewellyn & Harbour 2003, Riemer et al. 2007); with the exception of the study by Tilstone et al. (2010), who reported high concentrations of MAAs in the sea-surface micro-layer off the Iberian Peninsula, and by Llewellyn et al. (2012), who examined the variability in MAAs along a surface-water meridional transect in the Atlantic. Little is known about the abundance and composition of MAAs produced by phytoplankton in most of the world's open ocean waters or about their species-specific and spatial and seasonal photo-acclimation responses to UV exposure under various environmental conditions (Morrison & Nelson 2004).

The multidisciplinary SAZ-Sense cruise ('sensitivity of Sub-Antarctic Zone waters to global change') examined the microbial ecosystem structure and biogeochemical processes in the Sub-Antarctic Zone (SAZ) waters southwest and southeast of Tasmania and in the Polar Frontal Zone (PFZ) during the austral summer of 2007 (Bowie et al. 2011c). The aims of the SAZ-Sense study were to determine the factors driving productivity and carbon cycling in the SAZ waters, a major sink for atmospheric $CO_2$ (Metzl et al. 1999, Borges et al. 2008) and their sensitivity to future global change (see the special issue on the SAZ-Sense study: 'Biogeochemistry of the Australian Sector of the Southern Ocean', Bowie et al. 2011a). The Southern Ocean south of Tasmania is characterised by a high variability in the chlorophyll *a* (chl *a*) concentration between the west and east and between Sub-Antarctic and Polar Frontal waters (Trull et al. 2001). During the present study, high surface chlorophyll concentrations in the stratified waters in the SAZ southeast of Tasmania (chl $a > 1$ mg m$^{-3}$) contrasted with low chlorophyll concentrations in the PFZ (chl $a < 0.5$ mg m$^{-3}$ at 54°S) and in the SAZ southwest of Tasmania (chl $a \sim 0.8$ mg m$^{-3}$) (de Salas et al. 2011, Pearce et al. 2011). The large range of water types explored displayed strong differences in environmental conditions (light field, water column mixing, nutrients) and in the content and nature of particulate and dissolved materials and their light history, thus providing an ideal context to examine the photo-protective response of phytoplankton to different UV radiation conditions. The time scales of phytoplankton photo-adaptation processes under variable environmental conditions are not well known, but these are critical for ultimately understanding the impact of changes in light conditions at the surface and in the water column, which has important implications for regional and global primary productivity. In this study, we addressed the following questions: (1) What is the distribution of MAAs in the PFZ, sub-Antarctic waters and sub-tropical waters south of Tasmania? (2) How do natural phytoplankton assemblages in these regions respond to UV radiation exposure in terms of changes in absorption properties and MAA concentration and composition? (3) What are the kinetics and the driving factors of this response?

## MATERIALS AND METHODS

### Sampling strategy

The SAZ-Sense study was carried out during austral summer, between 20 January and 18 February 2007, south of Tasmania aboard the RV 'Aurora Australis'. Water samples were either collected from: (1) transect stations where a CTD-Rosette was deployed in the water column (0 to 200 m) or (2) process stations where the ship held position for several days while multiple CTD-Rosette casts were done at locations P1 in the SAZ-N southwest of Tasmania (SAZ-$N_W$), P2 in the PFZ (PFZ-S) and P3 in the SAZ-N southeast of Tasmania (SAZ-$N_E$) (Fig. 1). In what follows, we will use the abbreviations given in the brackets instead of process station numbers for clarity of location. At these stations, incubation experiments (abbreviated I*x*) were conducted in surface water for 1 to 2 d. Samples were collected at around the same time every day, in the early morning usually between 07:00 and 08:30 h (see Table 2), to minimise differences due to phytoplankton vertical migration patterns and diel photo-adaptation.

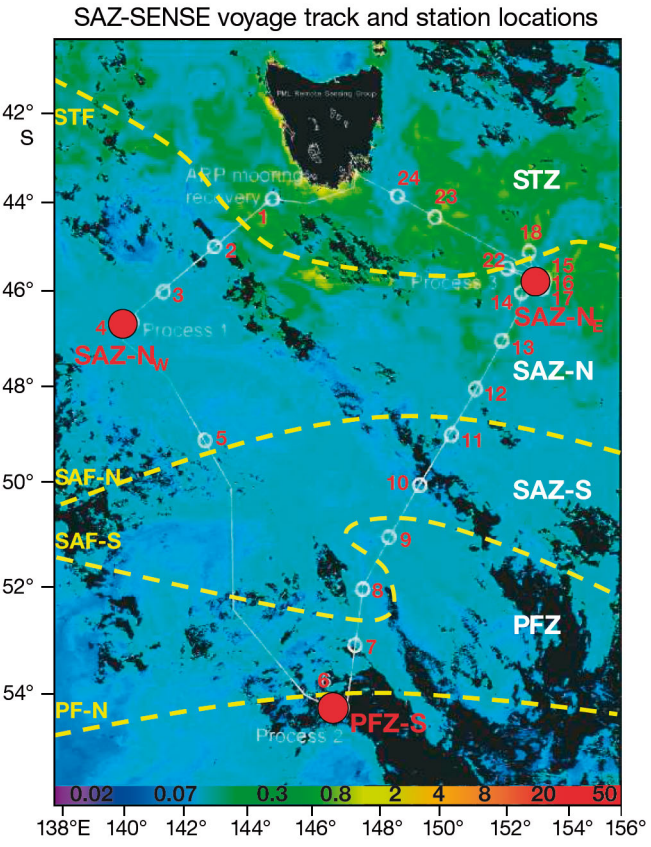


Fig. 1. Stations sampled during the SAZ-Sense cruise overlaid on a composite image of chlorophyll concentration (mg $m^{-3}$, the colour scale is logarithmic from 0.01 to 60 mg $m^{-3}$). Process stations are shown as red dots (SAZ-$N_W$: P1; PFZ-S: P2; SAZ-$N_E$: P3), and short stations are shown as white circles. Southern Ocean fronts (STF: Sub-Tropical Front; SAF-N: Sub-Antarctic Front North; SAF-S: Sub-Antarctic Front South; PF-N: Polar Front North) are shown in yellow, and water masses (STZ: Sub-Tropical Zone; SAZ-N: Sub-Antarctic Zone North; SAZ-S: Sub-Antarctic Zone South; PFZ: Polar Frontal Zone) are shown as white text. Most stations were sampled for mycosporine-like amino acids (MAAs) and the particulate absorption coefficient in the ultraviolet range as part of this study, except Stns 1, 3 and 8. Stn 20 (not shown) is located in a filament with higher chlorophyll concentration in the vicinity of SAZ-$N_E$ (slightly to the northwest)

### Incubation experiments

At each process station, surface-water samples were taken daily with two 20 l snatcher bottles early in the morning and placed in 1 l quartz glass flasks in 3 incubators (6 flasks per incubator) for between 9 and 11 h centred around solar noon (see Table 2 for details). The incubators were supplied with flow-through sub-surface seawater from the ship's underway supply to maintain the bottles at ambient temperature and were exposed to natural surface irradiance with no shading. Each incubator was covered with different materials to provide 3 UV radiation treatments: (1) UV-transparent Plexiglas: allowing transmission of UVB + UVA + PAR (photosynthetically active radiation) radiations (referred to in the text as UV + PAR), (2) Mylar-D: allowing only UVA + PAR radiations and (3) UV-opaque Plexiglas: allowing PAR only (see Fig. 2 for transmission spectra of the UV-transparent and UV-opaque Plexiglas used). Note that UV-opaque Plexiglas was not totally opaque in the close UVA region as transmission was equal to 7 and 61% at 380 and 390 nm, respectively. These incubations were repeated several times at each process station. Samples were collected at the start ($T_0$) and end of the incubation for the determination of particulate spectral absorption coefficients in the UV and visible wavelength ranges and the concentrations of MAAs in the particulate and dissolved fractions. Spectral UV and PAR were measured during the incubations using Trios-Ramses hyperspectral radiometers and a LICOR PAR sensor placed next to the incubators. It is worth noting that UV radiation received by phytoplankton cells inside the quartz flasks in each incubator was slightly lower than incident doses measured by the radiometers as these were placed outside of the incubators (e.g. due to the effect of Plexiglas screens). Cumulative daily

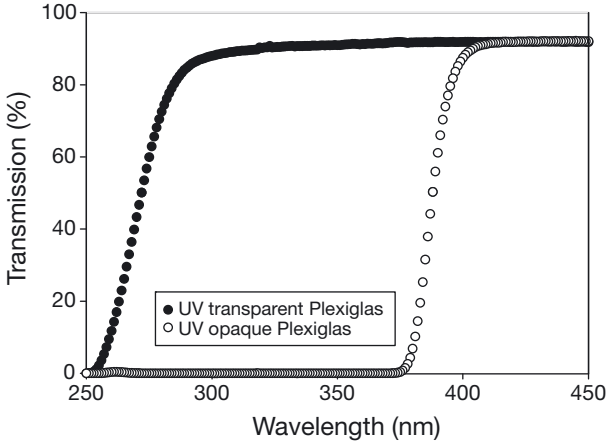


Fig. 2. Transmission of the ultraviolet (UV)-transparent Plexiglas and UV-opaque Plexiglas used for the incubation experiments between 250 and 450 nm

PAR and UVB radiation exposure were estimated by integration over the length of the incubations each day. Two day incubations were conducted 3 times during the cruise: once in the PFZ-S (I8) and twice in the SAZ-$N_E$ (I9 and I10). Because the particulate matter concentrations were low and the numbers of incubators and quartz flasks were limited, it was not possible to sub-sample at the end of the first day during experiment I8. This was done for I9 and I10, and the results for the intermediate sub-sampling (evening of the first day) are presented for I9. In addition, due to problems with surface-water flows before I6 in the PFZ-S, this incubation experiment started late (around 09:00 h) and thus was shorter than other incubation experiments. For this reason and simplicity of figures, the results from I6 are not presented. Paired *t*-test samples were employed to test for significant differences between light treatments. The *t*-test results are given as $t = x$ and $p = y$, where $t$ is the deviation of the sample mean from the normally distributed parametric mean to parametric standard deviation ratio and p is the *t*-test critical significance value.

### Vertical profiles

Samples were collected from 5 to 6 depths between 0 and 100 m using a 24 bottle Niskin rosette system coupled with a Seabird CTD for the determination of (1) particulate spectral absorption coefficients at UV and visible wavelengths and (2) the concentration of MAAs in the particulate fraction. The western transect was largely under-sampled due to poor weather conditions and time constraints. As a consequence, we were able to examine the spatial/latitudinal variability mainly along the eastern transect, from PFZ-S to Stn 24 (Fig. 1), because of the high sampling frequency.

## Optical and biogeochemical determinations

### Mycosporine-like amino-acids

For the determination of the particulate fraction, between 1 and 2 l of seawater was filtered through a Whatman GF/F 25 mm glass fibre filter (0.7 µm nominal porosity) and stored in liquid nitrogen until analysis in the laboratory back at Plymouth (PML). Filters were extracted in 2 ml of methanol by sonicating twice for 30 s, whilst being kept cool during extraction in an ice bath. Extracts were analysed by HPLC with reversed-phase C18 columns and gradient elution following the methods of Carreto et al. (2005). Identification of dominant MAAs was confirmed by retention time, UV/visible spectral matching and liquid chromatography-mass spectrometry (LC-MS) analysis on some duplicate samples with the highest diversity of MAAs. Response factors for MAA quantification were derived from MAAs isolated from culture extracts using preparative HPLC and verified by LC-MS, and quantified by UV/visible spectrophotometry using published extinction coefficients (Gröniger et al. 2000), as described by Llewellyn et al. (2012). More information on the LC-MS method can also be found in Llewellyn et al. (2012). In the present study, we decided to use 100% methanol instead of aqueous methanol for extraction of filters after testing extraction efficiencies on various natural phytoplankton samples. Extraction efficiencies were found to be overall higher across the whole range of MAAs with 100% methanol than with aqueous methanol, as shown in previous studies (e.g. Carreto et al. 2005).

For the determination of MAAs in the dissolved fraction (incubation experiments only), 1.5 l of seawater was filtered through Whatman GF/F 25 mm filters and the filtrate acidified to pH 2. Solid-phase extraction of dissolved MAAs was achieved using Isolute ENV+ cartridges without preconditioning (as recommended by the supplier). Filtering through 0.7 µm nominal porosity filters instead of 0.2 µm ('true dissolved') was driven by the need for relatively large volumes of filtered seawater in order to extract sufficient concentrations of MAAs and the time required to produce these filtrates through a given filter porosity (plus the associated

experimental bias linked to longer filtrations). However, most particulate material was retained by 0.7 µm filters in the waters sampled during the SAZ-Sense cruise: tests done with filters of different porosity (0.2 and 0.7 µm) at various sites showed <10% difference in the absorption coefficient at 320 nm and MAA concentration in the dissolved fraction. The ENV+ cartridges were stored at 4°C until analysis, which was done within a couple of months (previous tests on similar storage times in the laboratory have shown non-significant effects on MAAs). In the laboratory, MAAs were eluted from the cartridges with 4 ml of methanol; subsequently, the same process as described above was followed for the analysis of MAAs by HPLC. The volume of methanol required for elution was chosen after testing different volumes and was the optimum volume for elution of all MAAs (i.e. the elution efficiency did not increase when increasing the volume of methanol above 4 ml). MAA extraction efficiencies using solid-phase extraction were determined as follows: duplicate samples of known MAA composition and concentration (as analysed previously by HPLC) were diluted in 1.5 l of filtered seawater (where no MAAs were previously found), and the 'filtrate' was subsequently submitted to the same process as described above (filtrate acidified to pH 2, put through ENV+ cartridges, eluted with 4 ml methanol and finally analysed by HPLC). Solid-phase extraction efficiencies were equal to 26, 10, 19, 48 and 38% for shinorine, palythine, porphyra-334, palythenic-acid/M333 and palythene, respectively, and the associated standard deviations were equal to 1.5, 0.6, 1.6, 5.0 and 1.8. Correction factors were applied to 'eluted' concentrations to estimate the 'true' MAA concentration in the dissolved fraction. In contrast to the particulate fraction, mycosporine-glycine could not be extracted from the dissolved fraction using this method. These extraction efficiencies seem in some cases low but are higher than those estimated by the only other approach developed to date to quantify MAAs in the dissolved fraction by Whitehead & Vernet (2000), where the average measured extraction efficiencies were 7.2%.

Note that some MAAs such as usujirene and palythene are unstable in acidic medium (such as the one used in this method) and can yield to palythine by treatment with dilute hydrochloric acid (Carreto et al. 2005 and references therein), while other MAAs are stable in acidic medium. Carreto et al. (2005) showed that after standing at pH 3.15 (in mobile Phase A of the Carreto et al. 2005 method) at ambient temperature for 24 h, significant decreases in the concentrations of usujirene and palythene (9 and 12%, respectively) were accompanied by a significant increase in the palythine concentration (around 16%). Changes in the concentrations of other MAAs were small. However, usujirene and palythene were present in the particulate fraction samples only as a minor fraction in our study area (only in the SAZ-$N_E$). The time during which the MAAs were in the acidic medium before solid-phase extraction was kept to a minimum (<1 h), so that acidification occurred just before the samples were put through the ENV+ cartridges.

### Particulate absorption coefficient $a_p(\lambda)$

Seawater (1 to 2 l) was filtered through Whatman GF/F filters, and $a_p(\lambda)$ was measured from 290 to 750 nm in 1 nm increments using the quantitative filter technique with an Avantes spectrophotometer coupled with an optical fibre and a filter holder. The interior of the filter holder connected to the optical fibre facing the detector, was covered with reflective material to ensure that most of the scattered light arising from the filter was collected back into the optical fibre and hence quantified by the detector. The measurements were done onboard on fresh samples and within 5 to 10 min after the end of the filtration to minimise changes in the absorption properties in the UV range, as delays in measurements or freezing of samples have been shown to increase UV absorption (Laurion et al. 2003). Triplicate measurements were made on each filter and averaged. The path-length amplification effect by the filter (beta factor) was corrected following Bricaud & Stramski (1990, their Eq. 2, wavelength range: 380 to 750 nm) after a null-point adjustment by subtracting the average value measured at 750 nm (averaged across a 10 nm wavelength range: 745 to 755 nm) from all other wavelengths. The range of optical density of the sample on filter ($OD_f$) in our study was within the range of $OD_f$ values examined by Bricaud & Stramski (1990) (0.05 to 3). Note that we used a beta factor developed in the visible region, as to date there was no available estimation of the beta factor in the UV wavelength range for various mixed natural phytoplankton assemblages. Only one previous study (Laurion et al. 2004) examined the beta factor on diatom and dinoflagellate cultures in the UV wavelength range, and showed great variability between species, in particular when measurements were not done immediately after filtration. However, in the

absence of alternative methods for the determination of the particulate absorption in the UV wavelength range on natural samples, the quantitative filter technique remains the only available method. In the future, we strongly recommend a direct estimation of the beta factor in the UV wavelength range on different phytoplankton species and natural assemblages to provide more accurate estimates of the particulate absorption coefficient using this technique.

No corrections of the data presented were made for non-algal particulate material, as this was not determined on fresh samples using the present method due to time limitations during the research cruise. Parallel measurements of particulate absorption coefficients were carried out at some stations (up to 3 different depths per site) on frozen samples brought back to the laboratory from which the contribution of phytoplankton and non-algal particulate material were determined. The measurements showed that the non-algal contribution to the particulate absorption coefficient was low in the visible range (<10%, data not shown).

### Pigment concentration and composition

Seawater (1 to 2 l) was filtered through Whatman GF/F filters and stored in liquid nitrogen until analysis back in the laboratory in Hobart. For the incubation experiments, chl *a* and other phytoplankton pigment concentrations were determined by HPLC, using the extraction protocol described by Clementson et al. (2001) and using the method of Van Heukelem & Thomas (2001) for HPLC analysis. For the vertical profiles, chl *a* and other phytoplankton pigment concentrations were determined by HPLC following the method of Wright et al. (2010). The variability in species composition and abundance across the study area, as derived from phytoplankton pigment and microscopic determinations, is described in detail by de Salas et al. (2011). Some of this information will be used later in the discussion.

## RESULTS

### Environmental conditions

The SAZ was delimited in the north by the subtropical front around 45.5° S and in the south by the polar front around 53.5° S. The location of the stations relatively to the different water masses is given in Table 1 and on Fig. 1. Along the eastern transect (44 to 54° S, 146 to 154° E), the northern SAZ (SAZ-N) surface layer was characterised by temperatures ≥10°C and salinities of ~34.8, and the southern SAZ

Table 1. Station numbers, coordinates, corresponding water types, sampling dates and times, mixed layer depths ($Z_m$), euphotic depths ($Z_e$), surface chl *a* concentrations and surface chl *a*-specific mycosporine-like amino acid (MAA) concentrations during the SAZ-Sense survey. Mixed-layer depth was calculated as the first depth deeper than 10 m where the sigma-theta difference is >0.05 kg m$^{-3}$ from the near-surface value. Note that $Z_m$ was generally >60 m in most of the PFZ, SAZ-S and south of the SAZ-N (Stns 12 and 13), and <27 m north of the SAZ-N and in sub-tropical waters. STZ: Sub-Tropical Zone; SAZ-N: Sub-Antarctic Zone North; SAZ-S: Sub-Antarctic Zone South; PFZ: Polar Frontal Zone. Stns SAZ-$N_W$ and SAZ-$N_E$ are in the SAZ-N southwest and southeast of Tasmania, respectively, and PFZ-S is in the PFZ (see Fig. 1). AEST: Australian Eastern standard Time

| Station name | Coordinates (latitude south–longitude east) | Water type | Sampling date (in 2007) | Sampling time (AEST) | $Z_m$ | $Z_e$ | Surface chl *a* (mg m$^{-3}$) | Surface chl *a*-specific MAAs (mg mg$^{-1}$) |
|---|---|---|---|---|---|---|---|---|
| SAZ-$N_W$ | 46.46–140.35 | SAZ-N | 24 Jan | 08:02 | 46 | 56 | 0.97 | 0.95 |
| PFZ-S | 54.16–146.55 | PFZ | 4 Feb | 08:12 | 53 | 76 | 0.44 | 1.09 |
| Stn 7 | 53.01–146.83 | PFZ | 7 Feb | 02:10 | 64 | 85 | 0.35 | 1.67 |
| Stn 9 | 50.94–148.58 | PFZ | 8 Feb | 00:10 | 112 | 90 | 0.62 | 0.24 |
| Stn 10 | 50.00–149.44 | SAZ-S | 8 Feb | 13:28 | 67 | 81 | 0.40 | 0.43 |
| Stn 11 | 49.00–150.33 | SAZ-S | 9 Feb | 08:01 | 69 | 77 | 0.40 | 0.42 |
| Stn 12 | 48.03–151.22 | SAZ-N | 9 Feb | 21:25 | 83 | 35 | 1.18 | 0.82 |
| Stn 13 | 47.00–152.07 | SAZ-N | 10 Feb | 10:24 | 63 | 38 | 1.57 | 0.93 |
| Stn 14 | 45.99–152.91 | SAZ-N | 10 Feb | 17:07 | 18 | 42 | 0.75 | 1.91 |
| Stn 18 | 44.75–153.00 | SAZ-N | 13 Feb | 13:00 | 27 | 47 | 1.43 | 1.45 |
| Stn 20 | 44.94–152.40 | SAZ-N | 14 Feb | 08:11 | 25 | 27 | 1.38 | 2.54 |
| Stn 21 | 45.23–152.76 | SAZ-N | 14 Feb | 18:22 | 15 | 33 | – | – |
| Stn 22 | 45.27–153.01 | SAZ-N | 14 Feb | 21:19 | 23 | 44 | 1.17 | 1.68 |
| SAZ-$N_E$ | 45.51–153.65 | SAZ-N | 15 Feb | 18:33 | 19 | 35 | 1.52 | 1.81 |
| Stn 23 | 44.23–150.21 | STZ | 18 Feb | 18:01 | 17 | 61 | 0.70 | 0.46 |
| Stn 24 | 43.65–148.60 | STZ | 19 Feb | 14:48 | 23 | 61 | 0.47 | 1.38 |

(SAZ-S), by temperatures <10°C and salinities of 34.2 to 34.4. Stn 9 was located in a meander of polar waters pushing northwest within the SAZ-S. Stns 23 and 24 were positioned in sub-tropical waters influenced by the East Australian Current (EAC), with surface salinities >35.4 and temperatures >16°C. The water column was well mixed at the southernmost sites (the mixed layer depth, $Z_m$, was 112 m at Stn 9) and highly stratified southeast of Tasmania ($Z_m$ was ~20 m in the SAZ-$N_E$) (Table 1). An active mixing between warm/salty sub-tropical waters and cool/fresher SAZ waters was found in the northern part of the SAZ, as depicted by the variability within process stations in the SAZ-$N_W$ and SAZ-$N_E$. In the SAZ-$N_W$, I3 and I4 were likely influenced by the penetration of sub-tropical waters through the weak sub-tropical front, while I2 was in typical SAZ waters. In the SAZ-$N_E$, the mixing occurs with waters and eddies of the EAC extension. See Bowie et al. (2011b) for more details on the hydrography of the study area.

Nitrate and phosphate concentrations generally increased from north to south (Bowie et al. 2011b), and were limiting only in sub-tropical waters. Trophic conditions ranged from oligotrophic to eutrophic, with chl *a* concentrations varying from 0.2 mg $m^{-3}$ in the surface waters of the PFZ (PFZ-S) to a maximum of 2.5 mg $m^{-3}$ southeast of Tasmania (Stn 20). The euphotic depth ($Z_e$, depth where PAR is attenuated to 1% of its surface value) varied from 90 m at Stn 9 to 27 m at Stn 20 (Table 1). $Z_e$ was usually deeper than $Z_m$, except at Stns 9 (PFZ), 12 and 13 (south of the SAZ-N) where $Z_m$ was deeper than $Z_e$ by 22, 48 and 25 m, respectively. At the 3 process stations, incident light conditions (PAR, UVA and UVB radiations) were variable. Daily cumulative PAR doses varied from 6590 to 8659, 4226 to 8976, and 4533 to 10746 kJ $m^{-2}$ in the SAZ-$N_W$, PFZ-S and SAZ-$N_E$, respectively (Table 2). Daily cumulative UVB radiation doses ranged from 22 to 27, 17 to 34 and 14 to 41 kJ $m^{-2}$ in the SAZ-$N_W$, PFZ-S and SAZ-$N_E$, respectively. The maximum UVB/UVA ratio at solar noon was found to be between ~0.04 to 0.045 (SAZ-$N_W$ and PFZ-S) and 0.05 (SAZ-$N_E$).

## Spatial trends in particulate absorption coefficient and MAA concentration

### Particulate absorption coefficient

Particulate absorption coefficients present strong latitudinal and vertical gradients, which are discussed primarily for the eastern transect since the

Table 2. List of incubations of surface-water samples conducted during the SAZ-Sense cruise, with locations, sampling dates and times, lengths of the incubations (I), cumulative photosynthetically active radiation (ΔPAR, integrated over the length of the incubation), ultraviolet-A (UVA) and ultraviolet-B (UVB) radiation (ΔUVA and ΔUVB). Corresponding MAA production rates are also provided (ΔMAA in mg $m^{-3}$ normalised by ΔUVB in kJ $m^{-2}$, equivalent to the increase in MAA concentration under UVB relative to $T_0$ normalised by the cumulative UVB exposure over the length of the incubation). d: Day; see Table 1 for region abbreviations

| Process station (incubation no.) | Date (in 2007) | Incubation length (d) | Sampling time (start–end) | ΔPAR (kJ $m^{-2}$) | ΔUVA (kJ $m^{-2}$) | ΔUVB (kJ $m^{-2}$) | ΔMAA/ΔUVB |
|---|---|---|---|---|---|---|---|
| SAZ-$N_W$ (I2) | 24 Jan | 1 | 08:00–19:00 | 8659 | 724 | 27 | 0.0056 |
| SAZ-$N_W$ (I3) | 25 Jan | 1 | 08:00–19:00 | 7691 | 697 | 28 | 0.0009 |
| SAZ-$N_W$ (I4) | 26 Jan | 1 | 08:00–19:00 | 6590 | 594 | 22 | 0.0075 |
| PFZ-S (I5) | 1 Feb | 1 | 10:00–19:00 | 7160 | 596 | 23 | 0.0108 |
| PFZ-S (I7) | 3 Feb | 1 | 08:00–19:00 | 7367 | 708 | 29 | 0.0016 |
| PFZ-S (I8) | 4–5 Feb | 2 | 07:30 (d1)–19:00 (d2) | 4226 (d1)–8976 (d2) | 411 (d1)–884 (d2) | 17 (d1)–34 (d2) | 0.0086 |
| SAZ-$N_E$ (I9) | 12–13 Feb | 2 | 06:30 (d1)–19:00 (d2) | 4533 (d1)–5216 (d2) | 319 (d1)–550 (d2) | 14 (d1)–23 (d2) | 0.0261 |
| SAZ-$N_E$ (I10) | 15–16 Feb | 2 | 6:30–19:00 (d2) | 4729 (d1)–10746 (d2) | 511 (d1)–981 (d2) | 23 (d1)–41 (d2) | 0.0436 |

western transect was under-sampled due to adverse weather conditions. Examples of the vertical distributions of particulate absorption at 320 nm ($a_p$[320], an indicator of MAA expression) are shown in Fig. 3, and corresponding absorption spectra are given in Fig. 4 (PFZ-S, Stns 7 and 9 also in the PFZ, Stn 11 in the SAZ-S, and Stn 20 and SAZ-$N_E$). The corresponding chlorophyll vertical profiles are given for comparison. Note that $a_p$ is not normalised by chlorophyll concentration, as it includes algal and non-algal contributions (see 'Materials and methods'). However, the variability in $a_p$ magnitude and its spectral shape give valuable information described below. At the maximum depth, $a_p$(320) varied over a factor of 7: with a range of values of 0.015 (Stn 9) to 0.14 $m^{-1}$ (Stn 20). The vertical distributions of $a_p$(320) ranged from homogeneous low values in the PFZ and SAZ-S (PFZ-S, Stns 7, 9 and 11) to increasing values towards the surface in the SAZ-$N_E$. At Stn 20, the station with the highest chl *a* concentration over the study area, $a_p$(320) presented a sub-surface maximum coincident with the chl *a* maximum (which was dominated by diatoms; de Salas et al. 2011).

Three main patterns were observed in the spectral variability of the particulate absorption coefficient with depth, which changed by location (Fig. 4). (1) The first pattern was no change in the spectral shape in the UV and visible wavelengths in the PFZ, e.g. Stn 9, indicating the same type of phytoplankton over the $Z_m$ with no need for an increase in UV-absorbing compounds as phytoplankton were mixed down to 110 m. Note that the spectral shape was characteristic of a particle assemblage largely dominated by phytoplankton. (2) The second pattern was no change in the absorption properties in the visible wavelengths, contrasting with a slight increase in the absorption

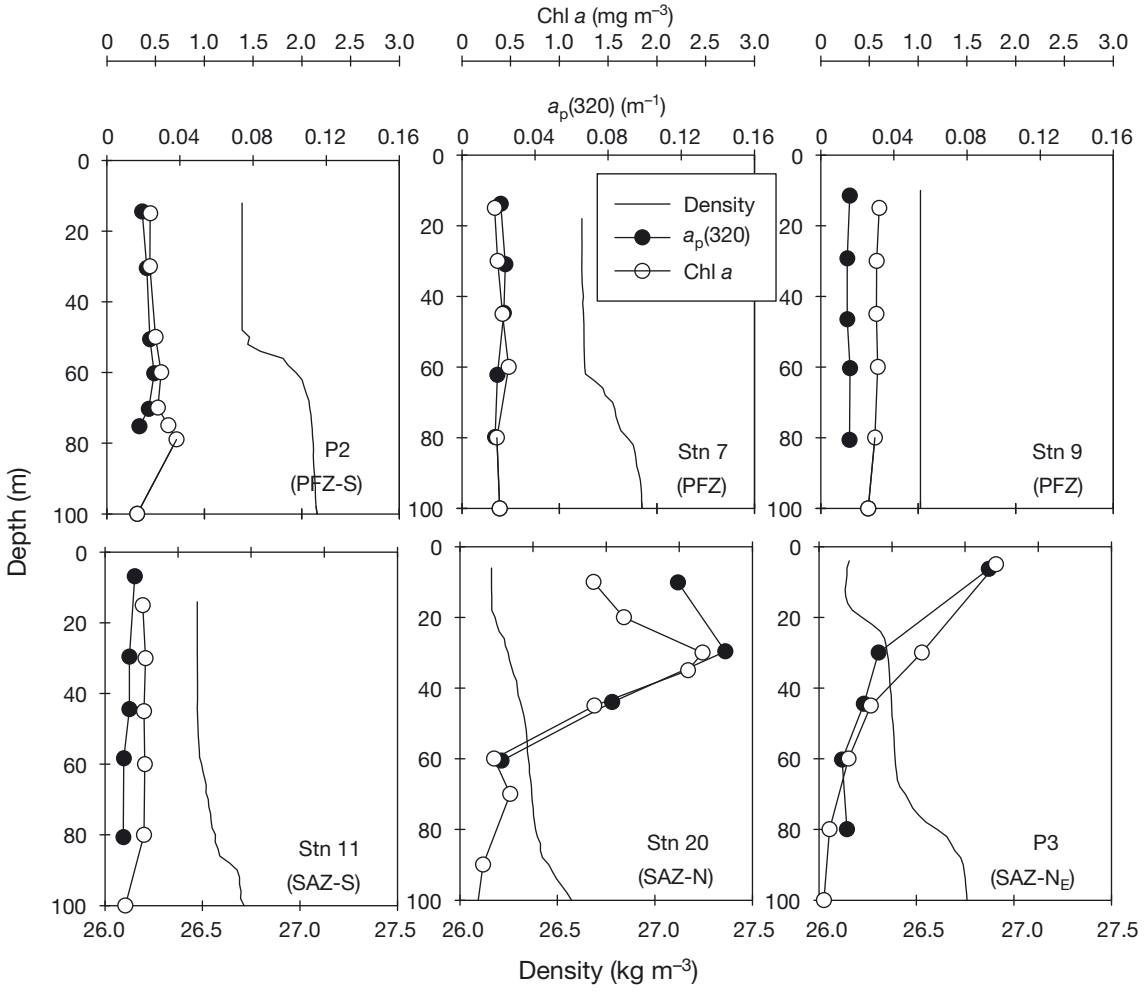


Fig. 3. Vertical profiles of particulate absorption coefficient at 320 nm [$a_p$(320)], chlorophyll *a* (chl *a*) concentration and density excess ($\sigma_\theta$) in the PFZ-S, at Stns 7, 9, 11 and 20 and in the SAZ-$N_E$ (see Table 1 for region abbreviations); 320 nm was chosen, as the particulate absorption coefficient was maximum at this wavelength over the study area

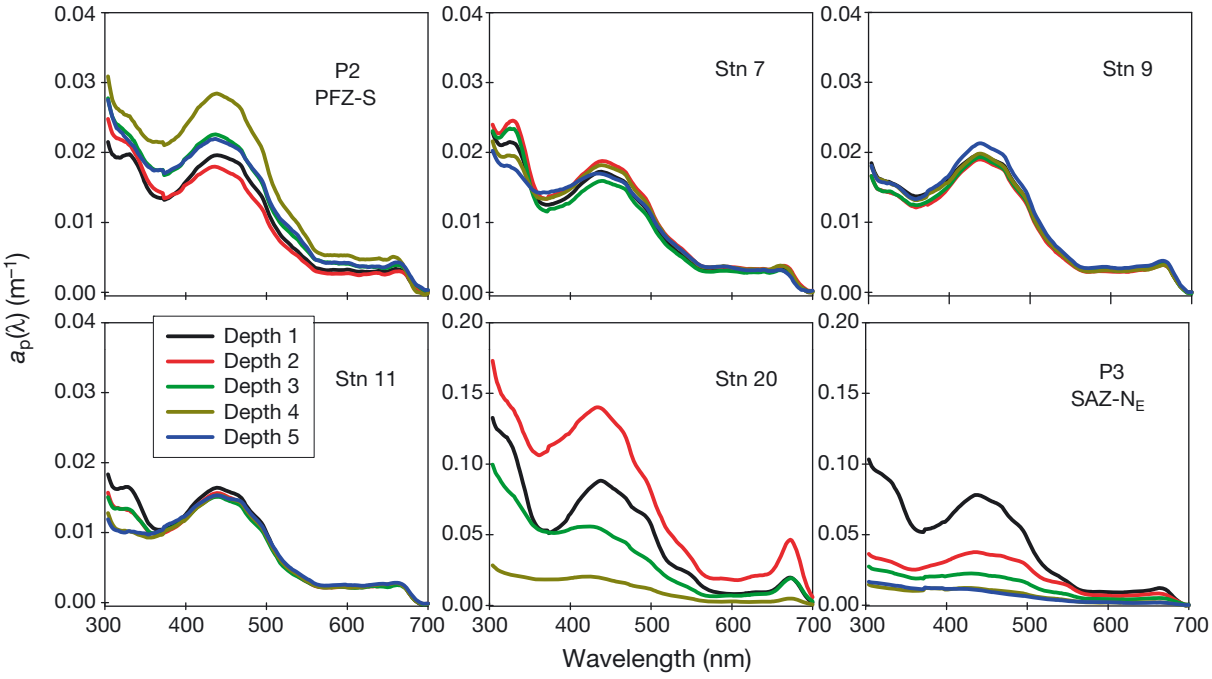


Fig. 4. Particulate absorption spectra in the PFZ-S, at Stns 7, 9, 11 and 20 and in the SAZ-$N_E$ (see Table 1 for region abbreviations) at different depths within the water column (see Fig. 3 for actual depths; Depth 5 not applicable for Stn 20). Note different scale for Stn 20 and SAZ-$N_E$

coefficient in the UV at depths closer to the surface (Stn 7 in the PFZ and Stn 11 in the SAZ-S), likely resulting from photo-acclimation of the same phytoplankton assemblage to UV radiation exposure in the near-surface layer through the production of UV-absorbing compounds. (3) The third pattern showed changes in absorption properties both in the UV and visible wavelengths, as for example at Stn 20 and SAZ-$N_E$, both located in the SAZ-N, as a consequence of simultaneous changes in the phytoplankton assemblage composition (as shown by pigment and microscopy analysis; de Salas et al. 2011) and its photoprotective response to increased UV radiation exposure at the surface. The spectral shape of $a_p$ also indicated a transition from phytoplankton-dominated material at the surface to material dominated by non-algal particles at deeper layers.

## MAA concentration and composition

Around 20 different MAAs were detected in samples collected at most stations. The 6 main MAAs were shinorine, porphyra-334, mycosporine-glycine, palythine, palythenic acid and palythene, which accounted for >80% of the total peak area of all MAAs. Because palythene was the least important of the 6 main MAAs, it is not shown in the respective figures. At the surface, the sum of these 6 MAAs in the particulate fraction (pMAA) varied by a factor of 20 across the study area, from 0.15 mg m$^{-3}$ in the PFZ (Stn 9) to 3.5 mg m$^{-3}$ in the SAZ-N (Stn 20) (Fig. 5). The vertical distribution of pMAAs ranged from well mixed with low concentrations in the PFZ and very low concentrations in the SAZ-S (Stns 10 and 11) to strongly stratified with high concentrations towards the surface in the SAZ-N. In sub-tropical waters (Stns 23 and 24) relative to SAZ-$N_E$, the decrease in surface pMAAs was 1 order of magnitude (0.32 mg m$^{-3}$ at Stn 23), which was due to a deepening of the mixed layer as a result of an EAC eddy. Unfortunately, the limited number of stations in sub-tropical waters does not allow us to make definitive conclusions for this water type. The surface chl *a*-specific concentration of MAAs varied by an order of magnitude along the eastern transect, from 0.24 mg mg$^{-1}$ in the PFZ (Stn 9) to 2.54 mg mg$^{-1}$ in the SAZ-N (Stn 20) (Table 1). By comparison, the chl *a*-specific concentration of MAAs was generally lower in the SAZ-N southwest of Tasmania (SAZ-$N_W$) than to the southeast (SAZ-$N_E$), and varied as a function of water type: from 0.52 mg mg$^{-1}$ in waters under sub-tropical influence (for I4 at $T_0$, see incubation results in the next section) to 1.7 mg mg$^{-1}$ in typical SAZ waters (for I2). The values observed are within the lower range of values from other studies on both freshwater and

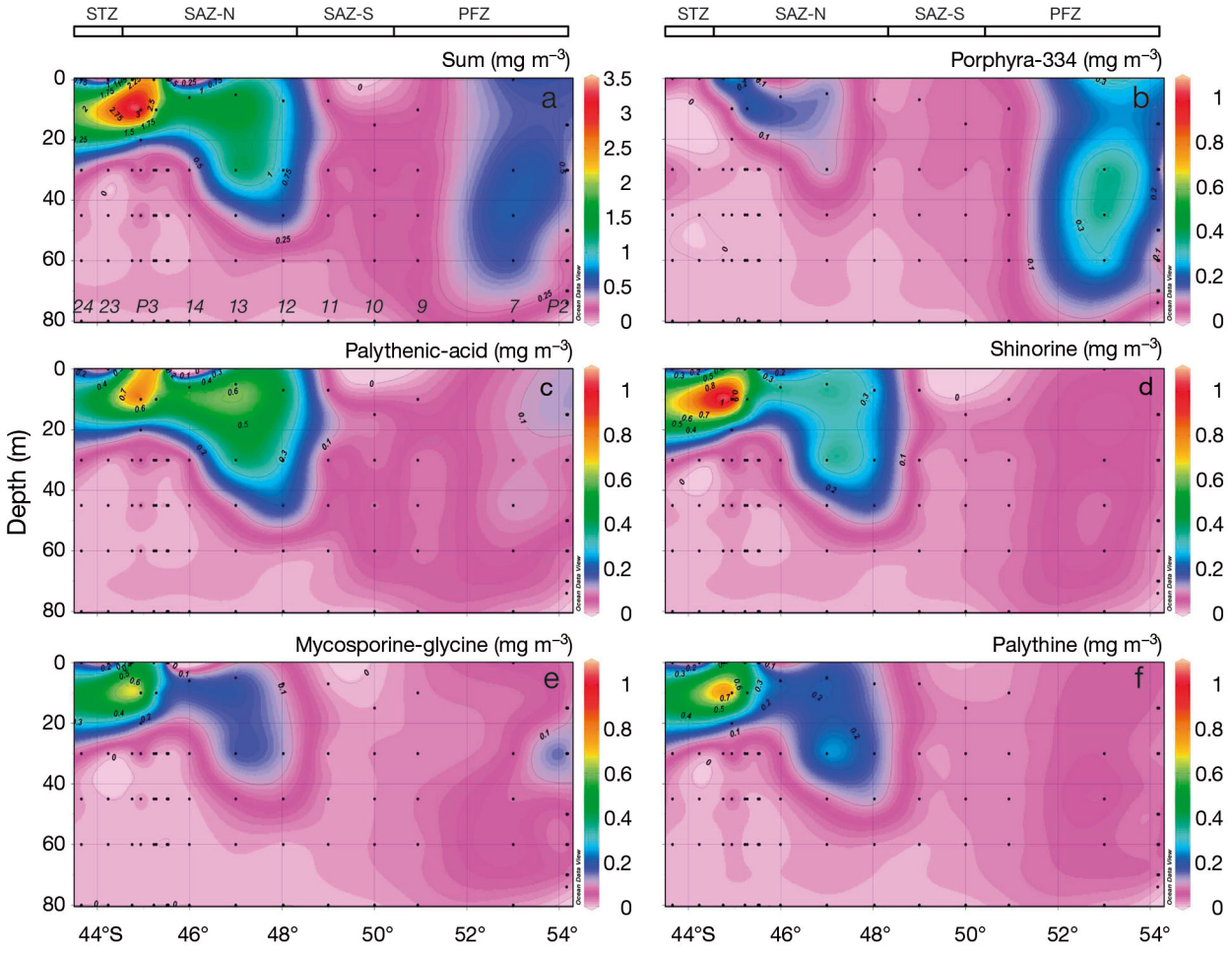


Fig. 5. Spatial distribution along the eastern transect (PFZ-S to Stn 24; see Table 1 for region abbreviations) in the surface layer (0 to 80 m) of (a) total MAAs (sum) in the particulate fraction (pMAA), (b) porphyra-334, (c) palythenic acid, (d) shinorine, (e) mycosporine-glycine and (f) palythine

marine phytoplankton (0 to 21 mg mg$^{-1}$; Laurion et al. 2002, see their Table 2, Riemer et al. 2007, Tilstone et al. 2010, Llewellyn et al. 2012, and references therein). The depth-dependent changes in pMAAs in stratified waters illustrate their photo-protective role, as previously reported for phytoplankton, zooplankton and coral species (Laurion et al. 2002, Shick & Dunlap 2002, Banaszak et al. 2006, Tartarotti & Sommaruga 2006).

The MAA composition within the particulate fraction strongly varied across regions along the eastern transect: the most abundant MAAs changed from porphyra-334 in the PFZ (>50% of pMAAs at Stn 7) to palythenic acid for most stations in the SAZ-S and SAZ-N (>30% of pMAAs in the SAZ-N$_E$), except at Stn 20 where shinorine was dominant (~30% of pMAAs; Fig. 5). Stn 20 also showed the highest pMAA and chl *a* concentrations, and diatoms dominated the phytoplankton assemblage. Shinorine was also the second most dominant MAA in the SAZ-N. The highest diversity of MAAs was in the north of the SAZ-N (especially in the SAZ-N$_E$ and surrounding waters), where some more stable forms of MAAs such as palythene and usujirene were present in significant concentrations only in this region (palythene was 0.11 and 0.17 mg m$^{-3}$ in the surface layer in the SAZ-N$_E$ and at Stn 20, respectively; data not shown). In sub-tropical waters (Stns 23 and 24), palythenic acid, shinorine, mycosporine-glycine and palythine were of equal importance (24, 22, 18 and 24%, respectively, at Stn 24). The vertical distribution of each of the MAAs showed contrasting patterns depending on the geographic location (Fig. 5). In the PFZ, the profiles were similar and rather homogeneous, with low concentrations within most of the mixed layer. By contrast, south of the SAZ-N (Stns 12

and 13), palythenic acid concentrations increased towards the surface, while other MAAs were either homogeneous with depth (e.g. shinorine) or exhibited a sub-surface maximum (e.g. palythine) associated with the chl *a* maximum. North of the SAZ-N (SAZ-$N_E$ and surrounding stations), the vertical distributions of the MAAs were similar and increased sharply towards the surface.

For all data, there was a significant linear relationship between the concentration of MAAs in the particulate fraction and $a_p(320)$ (Fig. 6; $y = 0.0266x + 0.0152$, $R^2 = 0.83$). The intercept is probably due to the contribution of non-algal particulate material to the total particulate absorption, which contributes <10% of $a_p$ at 440 nm over the SAZ (as determined from direct measurements done on separate samples). Increased self-shading at high concentrations likely explains the slight curvature of the relationship between $a_p(320)$ and pMAAs for higher MAA concentrations (Garcia-Pichel 1994). By contrast, Whitehead & Vernet (2000) found no such correlation during a large red tide in coastal waters off California.

## Phytoplankton response to different UV radiation treatments

### Particulate absorption coefficient

At the start of the incubations ($T_0$), $a_p(440)$ varied by a factor of 5 between the 3 sites (Fig. 7), from 0.013 $m^{-1}$ in the PFZ-S (I5) to ~0.065 $m^{-1}$ in the SAZ-$N_E$ (I9 and I10). The variation in $a_p(320)$ was slightly higher with 0.016 $m^{-1}$ in the SAZ-$N_W$ (I4) to 0.09 $m^{-1}$ in the SAZ-$N_E$ (I9). The $a_p(320)/a_p(440)$ ratio, an indicator of UV absorption relative to chl *a*, was <1 for I4 in the SAZ-$N_W$ (equal to 0.86) and >1 for all other samples in the SAZ and PFZ: between 1.2 and 1.9 in the PFZ-S (I8 and I7, respectively) and 1.3 and 1.4 in the SAZ-$N_E$ (I10 and I9, respectively). The phytoplankton response to different light treatments over 1 to 2 d differed depending on the location. In the SAZ-$N_W$ waters under sub-tropical influence (I3 and I4), there was no clear difference between light treatments, but a slight decrease in the absorption coefficient occurred over time for all incubations. In the SAZ-$N_E$, there was a slight change in particulate absorption properties at UV wavelengths as a function of light treatment. After 2 d, $a_p(320)$ increased by up to 21% under UV + PAR radiations for I9 (and by 9% at the end of the first day). In the PFZ-S, the absolute change in absorption properties in response to UV radiation was the highest, $a_p(320)$ increased by up to a factor of 2.3 under UV + PAR radiations after 2 d at I8. For this incubation experiment, the weather conditions were cloudy during the first day, but mostly sunny during the second day (daily UVB radiation exposures were 17 and 34 kJ $m^{-2}$, respectively; see Table 2). The large increase in $a_p$ during this incubation occurred at a range of wavelengths in the UVB and UVA ranges (300 to 400 nm) for samples exposed to UV + PAR radiations, but was limited to wavelengths <350 nm for samples under UVA + PAR radiations (although this increase was of the same amplitude at 320 nm as under UV + PAR radiations). This surprising response and its possible causes are discussed later. Under PAR only, $a_p(320)$ still increased by ~38%. During a previous experiment in the same region (I5), the changes were less marked between light treatments, with a 31% increase in $a_p(320)$ under UV + PAR radiations. At I7, still in the PFZ-S, $a_p(320)$ surprisingly decreased by ~40% for samples under UV + PAR radiations, in contrast to all other light treatments for which $a_p$ remained relatively constant.

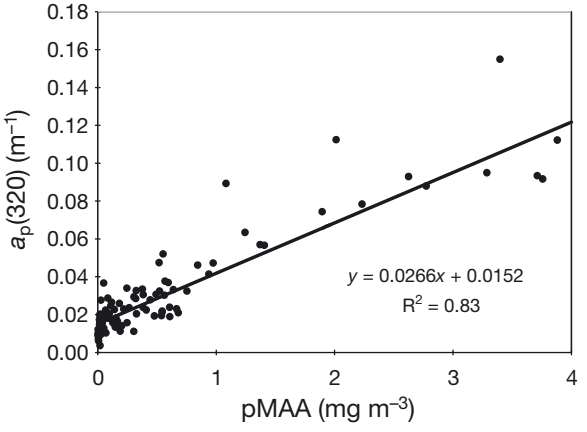


Fig. 6. Relationship between the particulate absorption coefficient at 320 nm ($a_p[320]$) and the total concentration of MAAs in the particulate fraction (pMAA)

### MAA concentration and composition (particulate and dissolved fractions)

At $T_0$, pMAAs in the incubated samples varied between 0.13 and 0.92 mg $m^{-3}$ in the SAZ-$N_W$ (I3 and I2), 0.14 and 0.69 mg $m^{-3}$ in the PFZ-S (I5 and I8) and 2.89 and 3.5 mg $m^{-3}$ in the SAZ-$N_E$ (I10 and I9) (Fig. 8). This range of variability is similar to that observed across the eastern transect (0.15 to 3.5 mg $m^{-3}$; Fig. 5). The most abundant MAA switched from porphyra-334 for a single incubation in the SAZ-$N_W$ (50% of pMAAs for I2, located in typical SAZ waters)

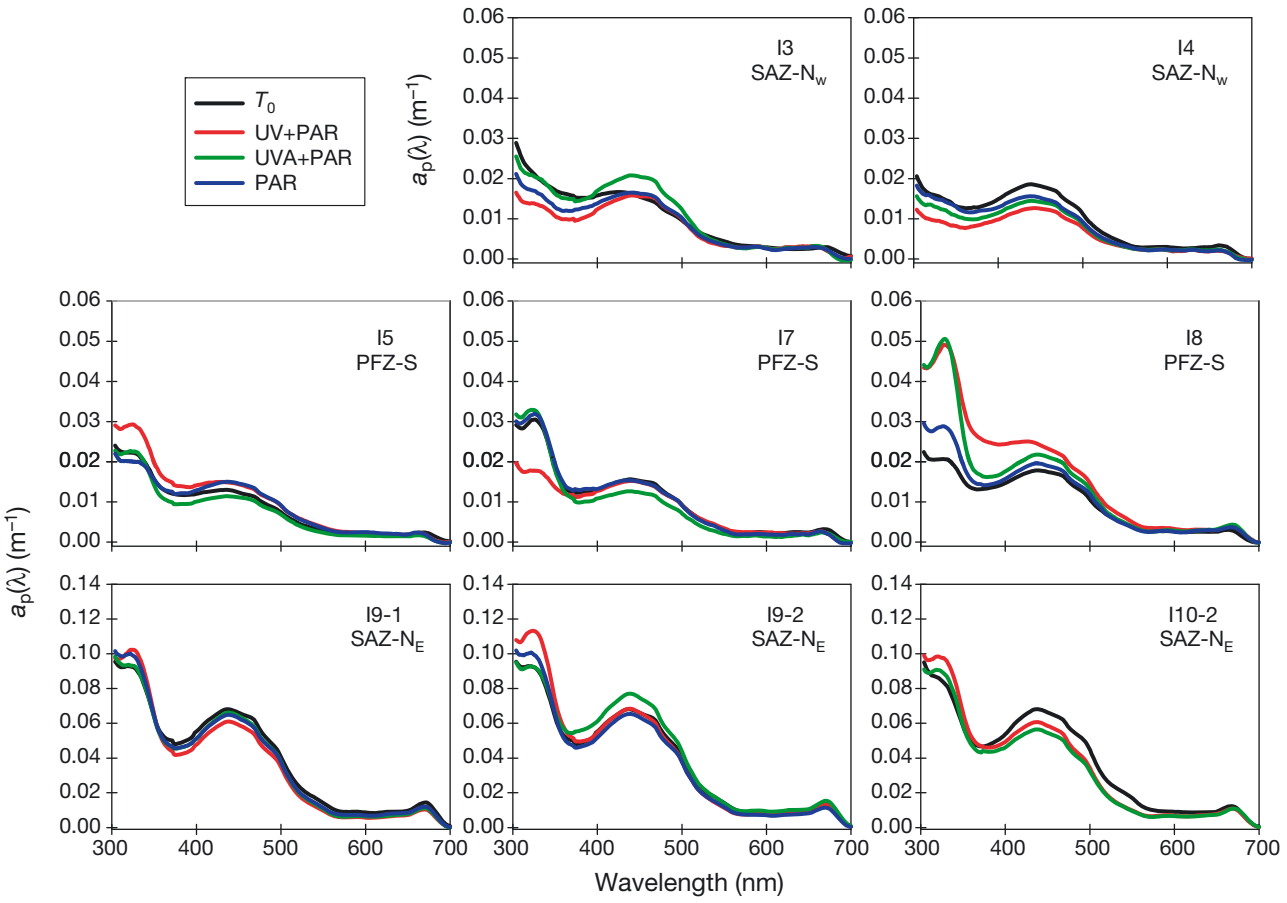


Fig. 7. Particulate absorption spectra of surface-water samples at $T_0$ and after exposure to 3 different UV radiation conditions (UV + PAR, UVA + PAR and PAR only) over 1 or 2 d (I9-2 and I10-2 only), during incubations (I) in the SAZ-N$_W$ (I3 and I4), PFZ-S (I5 to I8) and SAZ-N$_E$ (I9 and I10; note different scale). See Table 1 for region abbreviations

and all incubations in the PFZ-S (e.g. 48% of pMAAs for I8) to palythenic acid for all incubations in the SAZ-N$_E$ (e.g. ~32% of pMAAs for I9). For the 2 remaining incubations in the SAZ-N$_W$, influenced by the southward penetration of sub-tropical waters across the weak sub-tropical front, the dominant MAA was either mycosporine-glycine (36% of pMAAs for I3) or palythenic acid (31% of pMAAs for I4).

Changes in pMAAs were noticed in all 3 regions, with a maximum increase for samples exposed to UV + PAR radiations (Table 3). pMAAs increased by up to a factor of 2 in the SAZ-N$_W$ (I4), a factor of 2.7 (I5) or 1.4 (I8 after 2 d) in the PFZ-S, and a factor of 1.6 in the SAZ-N$_E$ (I10, after 2 d). The proportion of secondary MAAs systematically increased with UV radiation exposure at most process stations, with the largest increase under UV + PAR radiations. Over the whole sampling area (SAZ-N$_W$, PFZ-S and SAZ-N$_E$), paired *t*-tests showed that the changes in pMAAs between $T_0$ and under UV + PAR radiations were statistically significant ($p = 0.007$; Table 4). On a MAA composition basis, the increases were significant for palythenic acid and porphyra-334 ($p = 0.003$ and 0.044, respectively), but non-significant for other MAAs. When considering changes per region, the differences between $T_0$ and UV + PAR radiations appear statistically significant mainly in the SAZ-N$_W$ and PFZ-S and for palythenic acid ($p = 0.010$ and 0.015, respectively). In the SAZ-N$_E$, the increase in pMAAs was due to a slight increase in the concentration of palythenic acid after 1 d (I9) followed by an increase in concentration of most MAAs after 2 d (I9 and I10). However, these changes appear to be non-significant (see paired *t*-tests; Table 4). The production rates relative to UVB radiation exposure (the increase in MAA concentration under UV + PAR radiations relative to $T_0$ normalised by the cumulative UVB radiation exposure over the length of the incubation) were 0.0009 to 0.0075 mg m$^{-3}$ kJ$^{-1}$ UV m$^{-2}$ in the SAZ-N$_W$, 0.0016 to 0.0108 mg m$^{-3}$ kJ$^{-1}$ UV m$^{-2}$ in the PFZ-S and 0.0261 to 0.0436 mg m$^{-3}$ kJ$^{-1}$

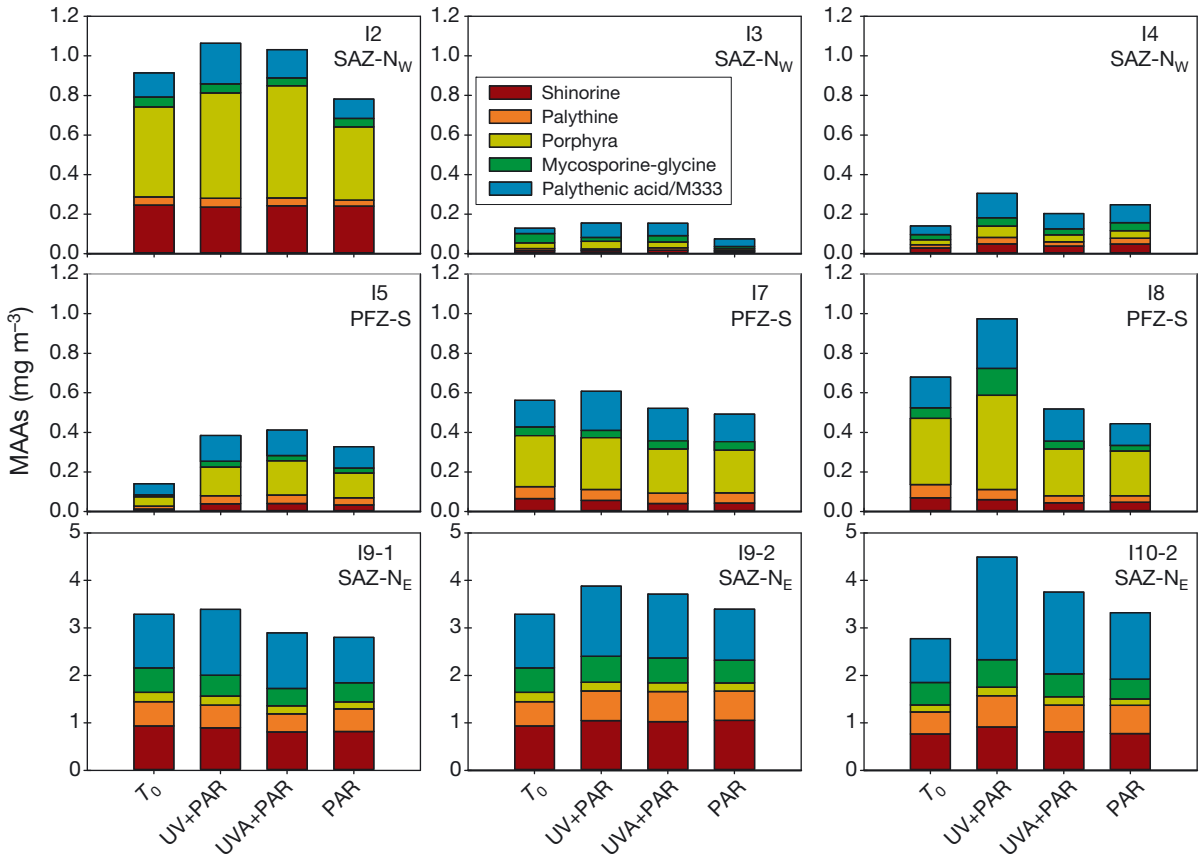


Fig. 8. Concentrations of different MAAs (porphyra-334, palythenic acid, shinorine, mycosporine-glycine and palythine) in the particulate fraction of surface-water samples at $T_0$ and after exposure to 3 different UV radiation conditions (UV + PAR, UVA + PAR and PAR only) over 1 or 2 d (I9-2 and I10-2 only) during incubations (I) in the SAZ-N$_W$ (I2 to I4), PFZ-S (I5 to I8) and SAZ-N$_E$ (I9 and I10; note different scale)

UV m$^{-2}$ in the SAZ-N$_E$. Note that these are minimum estimates as the UV radiation received by phytoplankton cells in the quartz flasks is slightly lower than the incident levels measured. pMAAs also decreased in some cases, as seen under both UVA + PAR radiation and PAR in the PFZ-S (for I7 and I8), which contrasted with the trend in particulate absorption coefficient.

The concentration of dissolved MAAs (dMAAs) accounted most of the time for <20% of the total concentration of MAAs (tMAAs = pMAAs + dMAAs), except for some incubations in the SAZ-N$_W$ (I3 and I4) and PFZ-S (I5 at $T_0$), where dMAAs did contribute >40% of tMAAs (Fig. 9, Table 3). In the SAZ-N$_W$ for I3, dMAAs/tMAAs ranged from 43 to 56% under UVA + PAR radiations and PAR, respectively. For I4, in the same region, dMAAs accounted for 21 to 52% of tMAAs under UV + PAR radiations and at $T_0$, respectively. dMAAs also reached 49 and 30% of tMAAs for I5 at $T_0$ and I8 under UVA + PAR radiations, respectively. The concentration of dMAAs either followed similar trends as pMAAs across all light treatments (e.g. I2 in the SAZ-N$_W$), or behaved differently (e.g. I8 in the PFZ-S). For most incubations, dMAAs under UV + PAR radiations were higher than under UVA + PAR radiations, which were in turn higher than under PAR, except for I4 and I8 (in this last case due to the UVA + PAR radiation treatment anomaly). By contrast, at $T_0$, dMAAs were either higher than for most other light treatments (I4, I5, or I9) or lower (I3 and I7). Note, however, that paired *t*-tests showed that the differences between $T_0$ and UV + PAR were not significant for dMAAs over the whole sampling area or for any specific region (Table 4).

Porphyra-334 was often the main MAA (or co-dominant with other MAAs) present in the dissolved fraction, even when not dominant in the particulate fraction (e.g. I9 and I10). The strongest increase in the contribution of dMAAs to tMAAs was noted for palythine or porphyra-334, depending on incubations. The maximal increase in the contribution of palythine was noted for I3, with >63% of tMAAs for all light treatments. The increase in the contribution of por-

Table 3. MAA concentrations in the particulate (p) and dissolved (d) fractions and relative contributions of dMAAs to total (t, particulate plus dissolved) MAAs, for each incubation and each light treatment, during the SAZ-Sense cruise. See Table 1 for region abbreviations

| Process station (incubation no.) | Date (in 2007) | Light treatment | pMAAs | dMAAs | dMAA/ tMAAs (%) |
|---|---|---|---|---|---|
| SAZ-$N_W$ (I2) | 24 Jan | $T_0$ | 0.91 | 0.05 | 6 |
| | | UV + PAR | 1.06 | 0.22 | 18 |
| | | UVA + PAR | 1.03 | 0.10 | 9 |
| | | PAR | 0.78 | 0.09 | 10 |
| SAZ-$N_W$ (I3) | 25 Jan | $T_0$ | 0.13 | 0.08 | 50 |
| | | UV + PAR | 0.16 | 0.11 | 46 |
| | | UVA + PAR | 0.15 | 0.09 | 43 |
| | | PAR | 0.08 | 0.08 | 56 |
| SAZ-$N_W$ (I4) | 26 Jan | $T_0$ | 0.14 | 0.13 | 52 |
| | | UV + PAR | 0.30 | 0.07 | 21 |
| | | UVA + PAR | 0.20 | 0.09 | 33 |
| | | PAR | 0.25 | 0.09 | 30 |
| PFZ-S (I5) | 1 Feb | $T_0$ | 0.14 | 0.13 | 49 |
| | | UV + PAR | 0.38 | 0.08 | 18 |
| | | UVA + PAR | 0.41 | 0.07 | 15 |
| | | PAR | 0.33 | 0.06 | 17 |
| PFZ-S (I7) | 3 Feb | $T_0$ | 0.56 | 0.07 | 12 |
| | | UV + PAR | 0.61 | 0.09 | 14 |
| | | UVA + PAR | 0.52 | 0.09 | 15 |
| | | PAR | 0.49 | 0.09 | 16 |
| PFZ-S (I8) | 4–5 Feb | $T_0$ | 0.68 | 0.10 | 14 |
| | | UV + PAR | 0.97 | 0.13 | 13 |
| | | UVA + PAR | 0.52 | 0.21 | 30 |
| | | PAR | 0.44 | 0.11 | 21 |
| SAZ-$N_E$ (I9) | 12–13 Feb | $T_0$ | 3.29 | 0.62 | 18 |
| | | UV + PAR | 3.88 | 0.52 | 14 |
| | | UVA + PAR | 3.71 | 0.43 | 12 |
| | | PAR | 3.40 | 0.35 | 11 |
| SAZ-$N_E$ (I10) | 15–16 Feb | $T_0$ | 2.78 | 0.44 | 16 |
| | | UV + PAR | 4.49 | 0.53 | 12 |
| | | UVA + PAR | 3.76 | 0.39 | 11 |
| | | PAR | 3.32 | 0.29 | 9 |

phyra-334 was maximal in waters under sub-tropical influence in the SAZ-$N_W$ (I3 and I4), and in the SAZ-$N_E$ (I9 and I10), with 37 to 71% of tMAAs. The observed increase in the contribution of porphyra-334 in the dissolved fraction, relative to the particulate fraction, is in agreement with observations made by Whitehead & Vernet (2000) following a red tide of dinoflagellates in coastal waters off California.

## DISCUSSION

The impact of UV radiation on a given phytoplankton assemblage depends on various factors, including exposure and vertical mixing conditions (Helbling et al. 1994, Neale et al. 1998c, Barbieri et al. 2002, Hernando & Ferreyra 2005), species composition and light history (Buma et al. 2006, Hernando et al. 2006) and nutrient availability (Lesser et al. 1994, Litchman et al. 2002). The contrasting environmental conditions and phytoplankton communities encountered during the SAZ-Sense cruise provided a unique opportunity to examine phytoplankton photo-protection mechanisms against harmful UV radiation through the production of MAAs. The present study showed: (1) the variability and diversity of MAAs over different trophic conditions and water masses from the PFZ to sub-Antarctic and sub-tropical waters, (2) the short time scale in phytoplankton photo-protective response (MAA production) to different UV light conditions and (3) the magnitude and variability of MAAs in the dissolved fraction. In what follows, we will examine the respective role of environmental and species-specific factors in the observed patterns in MAA distribution and photo-induction.

### UV radiation exposure and vertical mixing

Vertical mixing depth and rates will determine the residence time of phytoplankton cells at a certain depth and light condition and thus the cumulated UV radiation exposure (Neale et al. 1998c). The light conditions (intensity and quality) at a given depth are in turn a function of the inherent optical properties of particulate and dissolved materials. Previous studies have shown that vertical mixing can counteract the damaging effects of UV radiation (Cullen & Lesser 1991, Neale et al. 1998c, Hernando & Ferreyra 2005). Photo-inhibition and photo-damage are maximal when phytoplankton cells are rapidly mixed within the euphotic depth, and reduced when mixed well below the euphotic depth (Neale et al. 1998c).

Along the eastern transect, the mixed layer depth ranged from deep (generally >60 m) in most of the PFZ, SAZ-S and south of the SAZ-N (Stns 12 and 13) to shallow in the north of the SAZ-N (around SAZ-$N_E$) and in sub-tropical waters (<27 m). In most of the PFZ and SAZ-S, phytoplankton cells were likely to

Table 4. Statistical analysis (paired *t*-tests) of differences in particulate and dissolved MAAs between $T_0$ and UV + PAR radiation treatments during incubation experiments. N: number of samples; NA: not applicable. See Table 1 for region abbreviations, see Table 1. Significant p-values (<0.05) in **bold**

| Region (incubation no.) | MAAs | Particulate MAAs | | | Dissolved MAAs | | |
|---|---|---|---|---|---|---|---|
| | | N | *t* | p | N | *t* | p |
| All regions (I2–I10) | All MAAs | 11 | −3.34 | **0.007** | 9 | −1.04 | 0.328 |
| | Shinorine | 11 | −1.48 | 0.169 | 9 | 0.40 | 0.696 |
| | Palythine | 11 | −1.81 | 0.101 | 9 | −0.79 | 0.454 |
| | Porphyra | 11 | −2.30 | **0.044** | 9 | −0.66 | 0.528 |
| | Mycosporine-glycine | 11 | −1.11 | 0.291 | | NA | NA |
| | Palythenic acid | 11 | −3.86 | **0.003** | 9 | −1.56 | 0.162 |
| SAZ-$N_W$ (I2–I4) | All MAAs | 3 | −2.28 | 0.150 | 3 | −0.72 | 0.547 |
| | Shinorine | 3 | −0.30 | 0.791 | 3 | −0.91 | 0.459 |
| | Palythine | 3 | −1.14 | 0.373 | 3 | −0.60 | 0.609 |
| | Porphyra | 3 | −3.29 | 0.081 | 3 | −0.54 | 0.642 |
| | Mycosporine-glycine | 3 | 0.36 | 0.750 | | NA | NA |
| | Palythenic acid | 3 | −9.98 | **0.010** | 3 | −0.17 | 0.895 |
| PFZ-S (I5–I8) | All MAAs | 4 | −1.64 | 0.200 | | −0.76 | 0.500 |
| | Shinorine | 4 | −0.07 | 0.947 | 4 | −0.48 | 0.667 |
| | Palythine | 4 | −0.25 | 0.816 | 4 | −0.48 | 0.662 |
| | Porphyra | 4 | −1.24 | 0.304 | 4 | −0.78 | 0.490 |
| | Mycosporine-glycine | 4 | −1.12 | 0.345 | | NA | NA |
| | Palythenic acid | 4 | −5.06 | **0.015** | 4 | −0.92 | 0.426 |
| SAZ-$N_E$ (I9–I10) | All MAAs | 3 | −1.69 | 0.232 | 3 | 0.01 | 0.991 |
| | Shinorine | 3 | −1.25 | 0.337 | 3 | 3.01 | 0.204 |
| | Palythine | 3 | −1.39 | 0.300 | 3 | 0.06 | 0.965 |
| | Porphyra | 3 | −0.28 | 0.809 | 3 | 0.78 | 0.578 |
| | Mycosporine-glycine | 3 | −0.38 | 0.743 | | NA | NA |
| | Palythenic-acid | 3 | −2.08 | 0.173 | 3 | −1.86 | 0.314 |

be acclimated to lower average light intensities of PAR and UV radiation due to the deep mixed layers, and thus did not require significant photo-protection (as indicated by the low chl *a*-specific MAA concentrations, 0.24 mg $mg^{-1}$ at Stn 9). This is true despite the possible deeper penetration of UV radiation due to the low concentrations of particulate and dissolved matter (see $Z_e$ in Table 1). The same phytoplankton cells, however, can produce significant amounts of MAAs to protect against increased UVB radiations if constrained to surface light conditions long enough, as seen during the 2 d incubation experiment in the PFZ-S (I8) (see Tables 3 & 4). By contrast, in the stratified waters in the north of the SAZ-N, phytoplankton cells were probably already acclimated to high light intensities in the surface mixed layer and thus already contained large amounts of MAAs (as suggested by the high chl *a*-specific MAA concentration, e.g. 2.5 mg $mg^{-1}$ at Stn 20). When these cells were exposed to increased PAR and UV radiations (incubation experiments in the SAZ-$N_E$), the MAA concentrations slightly increased. However, we see the highest production rates relative to UVB radiation exposure over the study area in this region (Table 2). The region south of the SAZ-N (Stns 12 and 13) was characterised by an intermediate situation with deep mixed layers and relatively shallow euphotic depths (Table 1), but surprisingly significant MAA concentrations. This was probably due to factors other than UV radiation exposure and mixing conditions, such as shifts in phytoplankton composition (see following sub-section).

In the SAZ-$N_W$, the patterns were different in typical SAZ waters (I2) or under the influence of sub-tropical waters (I3 and I4). In SAZ waters, the MAA content of phytoplankton was relatively high (chl *a*-specific MAA concentration equalled 1.7 mg $mg^{-1}$ for I2 at $T_0$), and MAAs were further produced when constrained to high light intensities at the surface during incubation experiments under UV + PAR. This was similar to PFZ-S and SAZ-$N_E$, but with a different initial composition of MAAs, as a result of a different phytoplankton composition (de Salas et al. 2011). In waters under sub-tropical influence (I3 and I4), the initial MAA content was low and the impact of UV radiation (in terms of MAAs and $a_p$) was minor, as phytoplankton cells may have been photo-adapted to the high light intensities. It has been shown that tropical phytoplankton species and high irradiance (PAR) acclimated cells are more resistant

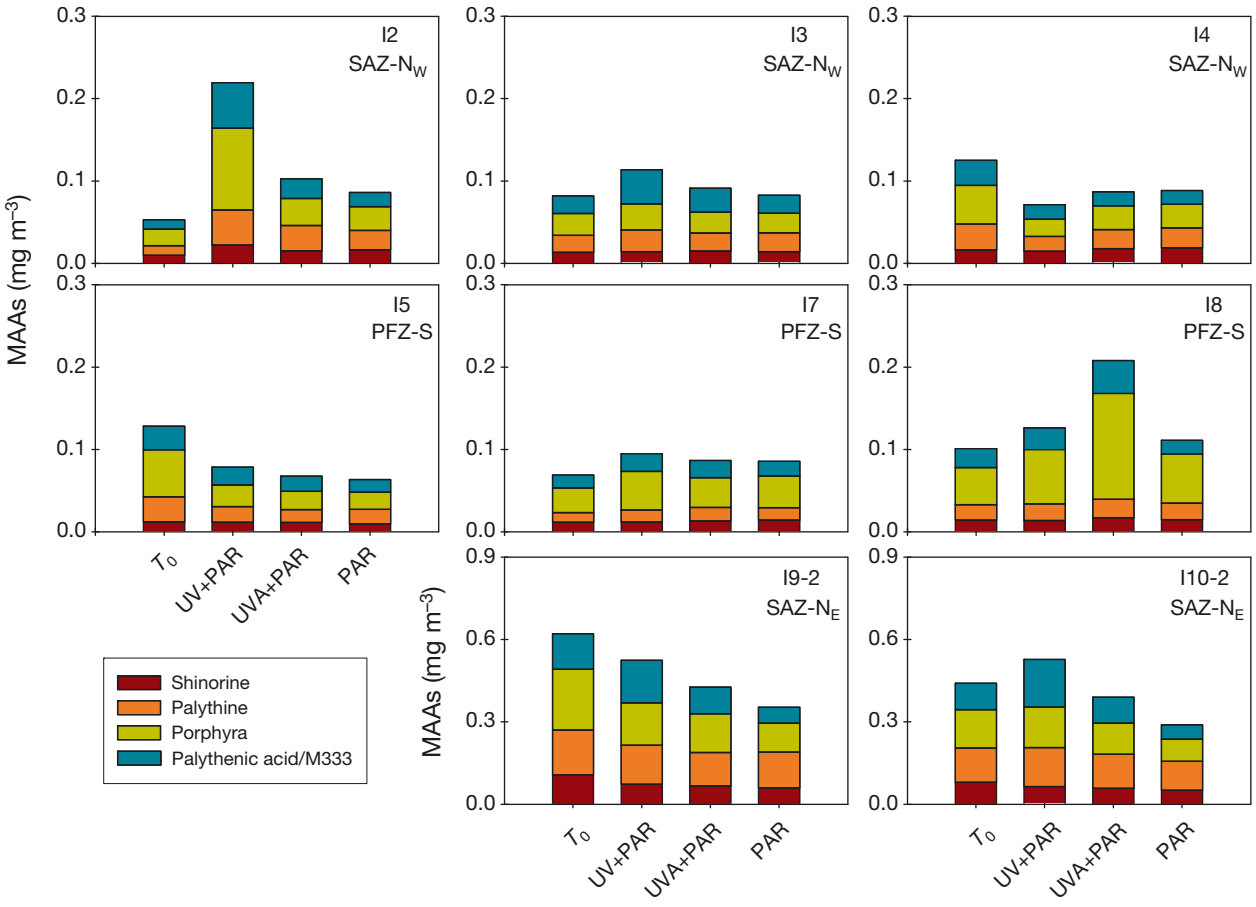


Fig. 9. Concentrations of different MAAs (porphyra-334, palythenic acid, shinorine and palythine) in the dissolved fraction of surface-water samples at $T_0$ and after exposure to 3 different UV radiation conditions (UV + PAR, UVA + PAR and PAR only) over 1 or 2 d (I9-2 and I10-2 only), during incubations (I) in the SAZ-$N_W$ (I2 to I4), PFZ-S (I5 to I8) and SAZ-$N_E$ (I9 and I10; note different scale)

to UV radiation in terms of photosynthesis than low irradiance acclimated cells and polar species (Villafañe et al. 2003, van de Poll et al. 2006, and references therein). Over long-term exposure to high irradiance, both in the visible and UV wavelengths range, phytoplankton develops alternative photoadaptation strategies, including repair processes and production of antioxidants.

Note that the sampling strategy during the SAZ-Sense cruise was not specifically designed for studying the effects of UV radiations, but to assess oceanographic parameters from the surface to 200 m. Thus, the vertical variability in the near-surface layer where most of the variability in UV radiation-related properties occurs cannot be fully described (which becomes critical at the stratified stations in the SAZ-N). For future studies focused specifically on the impact of UV radiation on phytoplankton, we recommend adaptation of the sampling strategy as a function of the optical properties of the water column/mixed layer depth, with a particular focus on the near-surface layer in stratified regions. Tilstone et al. (2010), for example, showed a strong variability in MAA concentrations near the surface and in the micro-layer off the Iberian Peninsula, underlying the strong requirement for alternative sampling strategies.

## Phytoplankton composition

Only some species are able to synthesise MAAs through photo-induction (Davidson et al. 1994, Hannach & Sigleo 1998, Jeffrey et al. 1999, Laurion et al. 2002, Callone et al. 2006, and references therein), and in some cases MAA composition is species specific. MAA-producing phytoplankton include dinoflagellates, cyanobacteria, prymnesiophytes, raphidophytes, cryptophytes and some diatoms (Davidson et al. 1994, Bandaranayake 1998, Neale et al. 1998a,

Jeffrey et al. 1999, Sinha et al. 2007, Carreto & Carignan 2011, Hernando et al. 2012). Some species have 'intrinsically' high concentrations of MAAs, while other species have low concentrations which can be induced by high PAR and/or UV radiation. They can either accumulate the same type of MAAs (for Antarctic diatom species: Hernando et al. 2002, 2012) or change their MAA composition (Hannach & Sigleo 1998, Callone et al. 2006, Hernando et al. 2012).

Along the eastern transect, some of the variability in MAA concentration and composition can be explained by shifts in the phytoplankton assemblage composition and their associated species-specific response to UV radiation. The switch from a porphyra-334 to a palythenic acid dominated MAA pool from the PFZ to the north of the SAZ is coincident with the appearance of peridinin-containing dinoflagellates (dinoflagellates-A) in the SAZ-N and cyanobacteria in the north of the SAZ-N (de Salas et al. 2011, Evans et al. 2011). Dinoflagellate species often contain inherently high concentrations of MAAs (Jeffrey et al. 1999) and have a high potential for MAA photo-induction under the appropriate light conditions (Callone et al. 2006, Laurion & Roy 2009, and references therein). Cyanobacteria can also produce high quantities of MAAs under enhanced UV radiation (Sinha & Hader 2008, and references therein). The presence of dinoflagellates likely explains the relatively high MAAs in the south of the SAZ-N (Stns 12 and 13) despite $Z_m$ being much deeper than $Z_e$. Fig. 10 shows the relationship between the chl *a* associated with dinoflagellates-A and cyanobacteria (dino-A + cyano, as derived by de Salas et al. 2011) and pMAAs in the SAZ-N (excluding Stn 20 as this station was dominated by diatoms). The correlation between MAAs and phytoplankton was mainly driven by dinoflagellates, but significantly improved when cyanobacteria were included. We observed 2 main trends: (1) for pMAAs <0.2 mg $m^{-3}$, there is a relatively linear increase in the concentration of MAAs as a function of the chl *a* associated with dinoflagellates-A and cyanobacteria, and (2) for pMAAs >0.2 mg $m^{-3}$, there appears to be the start of a 'saturation plateau', with the concentration of MAAs still increasing despite a proportionally smaller increase in the chl *a* associated with dinoflagellates-A and cyanobacteria. The first part of the relationship is probably due to the abundance of dinoflagellates-A and cyanobacteria being the main drivers of the MAA concentrations observed. The second part is likely a direct expression of MAA production by the same amount of dinoflagellates-A and cyanobacteria through photo-acclimation processes, and is mainly comprised of near-surface samples in stratified regions were cells are under increased UV radiation exposure, and thus require further photoprotection for survival.

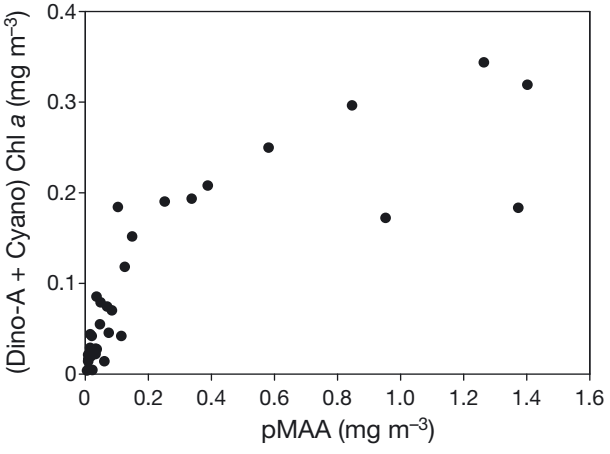


Fig. 10. Relationship between pMAAs (MAAs in the particulate fraction) and the chl *a* concentration associated with dinoflagellates-A (peridinin-containing dinoflagellates) and cyanobacteria in the SAZ-N (Stns 12 to SAZ-NE; see Table 1)

The presence of diatoms and their response to UV radiation exposure can explain some of the remaining patterns in MAA composition. Some diatoms can produce large amounts of MAAs, including shinorine and porphyra-334 (Karentz et al. 1991, Helbling et al. 1996, Riegger & Robinson 1997, Ingalls et al. 2010, Hernando et al. 2012). Diatoms were abundant in the SAZ-$N_W$, PFZ-S and at Stn 20 (de Salas et al. 2011), which explains the dominance of shinorine at Stn 20, porphyra-334 in the PFZ-S and both MAAs in the SAZ-$N_W$.

### Biotransformation processes of MAAs

The biotransformation processes for MAAs are a major factor in understanding the response of phytoplankton to UV radiation, but are still poorly understood. These biotransformation processes have been examined under different light treatments on phytoplankton cultures (Callone et al. 2006, Hernando et al. 2012, and references therein), but not on natural phytoplankton assemblages in the open ocean. The photo-protection process associated with MAAs occurs in 2 steps: (1) the biosynthesis of primary MAAs (mycosporine-glycine, porphyra-334 and shinorine) and (2) the metabolic transformation of these primary MAAs into secondary MAAs (all other MAAs), which often present increased stability (Portwich & Garcia-Pichel 2003, Shick 2004).

Phytoplankton cells accumulate preferentially the least 'acidic' secondary MAAs with a reduced noxious effect on cellular functions. The factors regulating the biotransformation pathways for MAAs range from the intensity and spectral quality of the incident light to the availability of assimilable nitrogen (Litchman et al. 2002, Doyle et al. 2005). Previous work has shown that mycosporine-glycine is the first MAA produced through the biosynthesis pathway and is the direct metabolic precursor of shinorine (Portwich & Garcia-Pichel 2003, Callone et al. 2006). Mycosporine-glycine is usually dominant in situations of nitrogen limitation, as this is the MAA which contains the fewest nitrogen atoms (Litchman et al. 2002). Carreto et al. (1990, 2001) also demonstrated that porphyra-334 is the precursor of palythenic acid, which can be in turn transformed into usujirene and palythene, as a result of metabolic changes induced by high light conditions.

The spatial and temporal variability in the distribution of MAAs during the SAZ-Sense study reflects these biotransformation processes under different environmental conditions and for different phytoplankton species. Primary MAAs such as porphyra-334 predominate in the deeply mixed/nutrient-rich waters of the PFZ (PFZ-S to Stn 9), as observed in Antarctic waters and other regions of the PFZ (Villafañe et al. 1995, Bracher & Wiencke 2000, Whitehead et al. 2001) and cultures of Antarctic species (Riegger & Robinson 1997). As shown during the incubation experiments, porphyra-334 also plays a major role in the photo-protective response to increased UV radiation in the PFZ (I8 in the PFZ-S) and typical SAZ waters southwest of Tasmania (I2 in the SAZ-$N_W$), where diatoms were abundant (de Salas et al. 2011). In agreement with our observations in the SAZ-$N_W$ and PFZ-S, Hernando et al. (2012) demonstrated on an Antarctic diatom culture (*Thalasiossira* sp.) that the concentrations of porphyra-334 and shinorine increased under exposure to UV + PAR radiations with an increase in the shinorine to porphyra-334 ratio after 24 h. The predominance of shinorine at Stn 20, where diatoms were dominant and the water column was stratified ($Z_m$ = 25 m), likely reflects the biotransformation process between porphyra-334 and shinorine due to the continuous exposure of diatom cells to increased UV and PAR radiations in the surface layer.

By contrast, secondary MAAs dominated the stratified waters in the SAZ-N southeast of Tasmania: palythenic acid was present over the whole region and more organic secondary MAAs such as palythine and palythene appeared in significant concentrations around SAZ-$N_E$. Incubation experiments also showed that the proportion of secondary MAAs such as palythenic acid increased significantly in the particulate fraction when phytoplankton cells were constrained to surface UVB radiation conditions across the whole region (SAZ-$N_W$, PFZ-S and SAZ-$N_E$). This is in agreement with the observations of Callone et al. (2006) who showed in cultures of the dinoflagellate *Alexandrium* sp. that cells exposed to high light intensities in the visible wavelengths transform primary MAAs such as porphyra-334 and mycosporine-glycine into secondary ones such as palythenic acid and palythene.

The response of phytoplankton in terms of absorption properties in the UV wavelength range provides further insight into the biotransformation processes for MAAs. In the PFZ-S (I8), the increase in $a_p$ in the UVA wavelength range under UV + PAR radiations disappears when the UVB radiation is filtered out, whilst the corresponding peak in the UVB wavelength range remains. UVB radiation probably acts as a trigger for the synthesis/transformation of some MAAs absorbing in the UVA wavelength region; this pattern would also reflect the findings of Klisch & Hader (2000) in culture studies of the dinoflagellate *Gyrodinium dorsum*. This increase in UV absorption corresponds with the increase in MAAs such as porphyra and palythenic-acid under UV + PAR radiations. These MAAs have relatively broad absorption spectra, with maxima at 334 and 337 nm, respectively. Other MAAs or UV-absorbing compounds, not quantified by the present HPLC method, might also play a role in the UVA absorption maximum. More detailed laboratory studies on species characteristic of the study area, including incubation experiments on cultures under different UV and visible radiation treatments, are required to improve our understanding of the mechanisms through which different environmental conditions trigger MAA production and changes in absorption properties in the UV.

### Intensity and spectral quality of incident light and the response time

The induction of MAAs is a function of the intensity and spectral quality of the incident PAR and/or UV radiation, with a spectral dependence which can vary between species (Carreto & Carignan 2011, and references therein). The production of MAAs can be induced by higher PAR intensities (Neale et al. 1998a, Moisan & Mitchell 2001, Buma et al. 2006, Callone et al. 2006), UVA (Riegger & Robinson 1997,

Hannach & Sigleo 1998, Klisch & Hader 2000) and/or UVB radiation (Marchant et al. 1991, Riegger & Robinson 1997, Hannach & Sigleo 1998, Klisch & Hader 2000, Laurion & Roy 2009). During the present study, the production of MAAs by phytoplankton is mainly induced by UVB radiation and to a lower extent by UVA radiation (Fig. 8), as also seen through changes in absorption properties in the UV wavelengths. This is in agreement with previous studies conducted on dinoflagellates, prymnesiophytes and cyanobacteria (Carreto & Carignan 2011, and references therein). Under PAR only, minimal concentrations of MAAs were observed with sometimes lower values than at $T_0$, which is probably due to a loss of MAAs by phytoplankton through transfer from the particulate to the dissolved fraction and/or possible subsequent degradation. The systematic increase of pMAAs after 2 d for all light treatments in the SAZ-$N_E$ shows that phytoplankton cells will ultimately accumulate MAAs over longer periods of time.

The present study shows that phytoplankton can respond to increased UV radiation on a time scale of hours through the fast synthesis/biotransformation of MAAs, which has also been reported for dinoflagellate cultures (Callone et al. 2006, and references therein) and Antarctic species including diatoms and the prymnesiophyte *Phaeocystis antarctica* (time scales ranging from hours to days; Riegger & Robinson 1997, Hernando et al. 2012). The MAA photo-induction rates relative to UVB radiation exposure were highest in the SAZ-$N_E$ after 2 d (Table 2), where dinoflagellate cells were able to produce large amounts of MAAs. Other studies have shown different phytoplankton species to require a longer time period before the induction of MAAs (e.g. 2 wk for a diatom culture [Zudaire & Roy 2001] or >4 wk for dinoflagellate and diatom cultures [Laurion & Roy 2009]). The differences in the photo-induction kinetics of MAAs between these different studies are probably due to species differences, physiological and photo-acclimation state and/or environmental conditions. Note that over the 2 d incubations, the effect of UV radiation is not assumed to be linear from Day 1 to Day 2. Various photo-acclimation and repair processes can occur overnight and lead to partial or full recovery. The present study does not unfortunately give us access to these night-time processes, but still brings valuable information on longer term (2 d) trends in phytoplankton response to UV radiation, which is complementary to the information provided by 1 d incubations. For the future we recommend incubations of several days to weeks, with intermediate sampling at the end of each day, to better understand the long-term effects of UV radiation on phytoplankton. Over longer time periods, phytoplankton species can develop alternative photo-adaptation strategies against UV radiation (Zudaire & Roy 2001, and references therein). It is also important to emphasise that short-term experiments of limited water volumes in incubators, although providing a better understanding of the mechanisms of phytoplankton photo-acclimation processes, usually overestimate the impact of UV radiation. These experiments restrict water movements and do not take into account the interactions between the different trophic levels that are accounted for in mesocosm experiments (see the special issue on 'UV effects on aquatic and coastal ecosystems', Kelly & Ullrich 2006).

### Particulate absorption coefficient in the UV

The differences in the UV particulate absorption response between incubation experiments seen in the PFZ-S can be the result of environmental factors or experimental artifacts. For I5, the less marked changes between light treatments (31% increase in $a_p$[320] under UV + PAR radiations) were possibly due to the shorter incubation time (Table 1) and cloudy weather conditions (daily UVB radiation of 23 kJ $m^{-2}$). For I7, the $a_p$(320) decrease by ~40% for samples under UV + PAR radiations, in contrast to all other light treatments for which $a_p$ remained relatively constant, could be due to: (1) an experimental artifact, as $a_p$ increased in the UV under UV + PAR radiations for all other incubation experiments in the PFZ-S (including I6; data not shown) and is not reflected in the MAA concentrations, or (2) the phytoplankton assemblage, in this specific quartz flask, being under stress for some unknown reason (concurrent pigment measurements showed that phytoplankton composition did not change during this short time period).

The differences between the particulate absorption in the UV wavelength range and pMAAs can be explained by several factors. Firstly, the variability in particulate absorption provides an 'integrated view' and reflects the contribution of all MAAs present (>20 identified by HPLC) and other UV-absorbing compounds not extracted or identified by the HPLC method, while the pMAA concentration presented in this study includes only the 6 main representative MAAs. Secondly, MAAs are likely to be concentrated or packaged around the UV radiation-sensitive organelles to increase photo-protection, and the level of packaging of MAAs can differ between cells and

species, and under different environmental conditions (Laurion et al. 2004). A higher packaging of the same amount of MAAs around sensitive targets in phytoplankton cells would be associated with a decrease in UV absorption. To date, no study has examined the level of packaging of MAAs as a function of light and physiological state under natural conditions. This type of study would provide further insights in its role in phytoplankton photo-protection processes, and is strongly recommended for future research. Finally, the possible release of packaged MAAs during filtration within the matrix of the filter without going into the dissolved fraction cannot be excluded, in particular for samples in which dinoflagellates are dominant (Laurion et al. 2003). This fraction of MAAs would still be quantified by HPLC as part of the pMAA fraction, but would lead to higher than expected values in $a_p$ in the UV region.

### MAAs in the dissolved fraction

Phytoplankton can release MAAs into the dissolved fraction through exudates as shown in studies using culture material (Vernet & Whitehead 1996), in coastal and open-ocean waters (Whitehead & Vernet 2000, Tilstone et al. 2010, Basu et al. 2011, Kitidis et al. 2011) and in Antarctic waters (Norman et al. 2011, and references therein), where they can represent up to 10% of the UV absorption coefficient in the dissolved fraction (Whitehead & Vernet 2000). MAAs can be linked to extracellular oligosaccharides as observed in some cyanobacteria and dinoflagellates (Vernet & Whitehead 1996, Carreto & Carignan 2011). Only one previous study directly quantified the concentration of MAAs released into the dissolved fraction using a chemical method (Whitehead & Vernet 2000). Other studies relied only on their absorption signature in the UV, including Tilstone et al. (2010) where the concentration of MAAs in the dissolved fraction was estimated using the absorption peak in the UV and the known extinction coefficients of MAAs.

We found that samples with a high proportion of dMAAs in the tMAAs in the SAZ-$N_W$ were from stations under the influence of sub-tropical waters (I3 and I4), where phytoplankton might be under stress (e.g. due to large changes in nutrients or temperature) and release MAAs (Vernet & Whitehead 1996, Whitehead & Vernet 2000). As highlighted by Laurion et al. (2003), a possible extracellular release and subsequent loss of the water-soluble MAAs during the filtration process cannot be ruled out either. The filtrations were done under low pressure, and the measurements were done immediately after the filtrations to minimise this loss. However, this may still have happened, as for example for I8 under UVA+PAR radiations, where dMAAs were unexpectedly much higher than in other treatments and in turn pMAAs were lower than at $T_0$.

Our understanding of the coupling between the particulate and dissolved phases is hampered by the fact that some dissolved MAAs can be degraded through photo-chemical processes or re-used in the microbial loop (Vernet & Whitehead 1996, Whitehead & Vernet 2000, Kitidis et al. 2011), and these processes are likely to be dependent on the chemical properties of each MAA. Most MAAs are rather stable compounds in seawater and can remain in the dissolved fraction for 2 wk after sampling (Vernet & Whitehead 1996). Conde et al. (2007) showed that porphyra-334, shinorine and palythine are highly photo-stable compounds in aqueous solution, and of the 3, palythine is the most photo-stable. Some MAAs can undergo photo-sensitisation in a seawater medium, however (Whitehead & Hedges 2005). Mycosporine-glycine, for example, is a rather unstable MAA under aerobic conditions (Carreto & Carignan 2011, and references therein). The higher photo-stability of palythine and porphyra-334 likely explains why these MAAs were found in greater proportions in the dissolved fraction in the SAZ-region, whilst the instability of mycosporine-glycine under aerobic conditions might be the reason it was not detected. Further studies are required into the photostability and photo-sensitisation of MAAs in the dissolved fraction under different environmental conditions and UV radiation treatments.

## CONCLUSIONS

The present study provides insight into the factors driving changes in the spatial distribution of MAAs in the SAZ, as well as in their production rates and fractionation into particulate and dissolved pools. Differences in exposure to UV radiation and PAR, mixing conditions, phytoplankton species composition and photo-acclimation state contributed to the observed patterns in MAA concentration and composition. Across the PFZ, SAZ and sub-tropical waters south of Tasmania, the primary source of variability was UV radiation exposure and vertical mixing conditions: the highest MAA concentrations and diversities were observed in the stratified waters to the southeast of Tasmania. The second

most important source of variability was due to shifts in the phytoplankton species, also closely driven by environmental conditions (including vertical mixing), and species-specific responses to UV radiation exposure. Finally, UV radiation exposure history (during the previous weeks) is also critical for a better understanding of the impact of increased UV radiation levels, as over the long term, phytoplankton can develop alternative photo-protection strategies. Similar studies in other regions of the world's oceans are recommended and will provide a better understanding of the ubiquity of the role of MAAs in phytoplankton photo-acclimation processes and photosynthesis. More coupled kinetic studies on the production of different MAAs by phytoplankton, their release in the dissolved fraction and their subsequent degradation (chemical or biological) are required, on cultures of key species found in the study area and in *in situ* conditions, for a better understanding of phytoplankton photo-protection strategies in marine ecosystems.

*Acknowledgements*. The authors thank Isabel Cook for advice on the set-up of the HPLC method for MAA analysis, David White for LC-MS identification of MAAs and the crew of the RV 'Aurora Australis' for their assistance at sea. We also acknowledge Simon Wright for providing chlorophyll *a* and pigment data for the vertical profiles. Brian Griffiths is especially acknowledged for providing the opportunity for K.O. to participate in the SAZ-Sense cruise. The satellite image (Fig. 1) is courtesy of the Natural Environment Research Council (NERC) Earth Observation Data Acquisition and Analysis Service (NEODAAS, www.neodaas.ac.uk) at the Plymouth Marine Laboratory. The research was financed by the Marie Curie fellowship 'UVphytoMAA' from the European Union (Contract No. 024823). G.H.T. and G.F.M. were financed by the NERC contract, Oceans 2025.

## LITERATURE CITED

Banaszak AT, Santos MG, LaJeunesse TC, Lesser MP (2006) The distribution of mycosporine-like amino acids (MAAs) and the phylogenetic identity of symbiotic dinoflagellates in cnidarian hosts from the Mexican Caribbean. J Exp Mar Biol Ecol 337:131–146

Bandaranayake WM (1998) Mycosporines: Are they nature's sunscreens? Nat Prod Rep 15:159–172

Barbieri ES, Villafañe VE, Helbling EW (2002) Experimental assessment of UV effects on temperate marine phytoplankton when exposed to variable radiation regimes. Limnol Oceanogr 47:1648–1655

Basu S, Matondkar SGP, Furtado I (2011) Enumeration of bacteria from a *Trichodesmium* spp. bloom of the eastern Arabian Sea: elucidation of their possible role in biogeochemistry. J Appl Phycol 23:309–319

Borges AV, Tilbrook B, Metzl N, Lenton A, Delille B (2008) Inter-annual variability of the carbon dioxide oceanic sink south of Tasmania. Biogeosciences 5:141–155

Bowie AR, Griffiths FB, Dehairs F, Davis DM (eds) (2011a) Biogeochemistry of the Australian sector of the Southern Ocean. Deep-Sea Res II 58(Spec Issue):2051–2316

Bowie AR, Griffiths FB, Dehairs F, Trull TW (2011b) Oceanography of the subantarctic and polar frontal zones south of Australia during summer: setting for the SAZ-Sense study. Deep-Sea Res II 58(Spec Issue): 2059–2070

Bowie AR, Trull TW, Dehairs F (2011c) Editorial: estimating the sensitivity of the subantarctic zone to environmental change: the SAZ-Sense project. Deep-Sea Res II 58(Spec Issue):2051–2058

Bracher AU, Wiencke C (2000) Simulation of the effects of naturally enhanced UV radiation on photosynthesis of Antarctic phytoplankton. Mar Ecol Prog Ser 196:127–141

Bricaud A, Stramski D (1990) Spectral absorption coefficients of living phytoplankton and nonalgal biogenous matter: a comparison between the Peru upwelling area and the Sargasso Sea. Limnol Oceanogr 35:562–582

Buma AGJ, Wright SW, van den Enden R, van de Poll WH, Davidson AT (2006) PAR acclimation and UVBR-induced DNA damage in Antarctic marine microalgae. Mar Ecol Prog Ser 315:33–42

Callone AI, Carignan M, Montoya NG, Carreto JI (2006) Biotransformation of mycosporine like amino acids (MAAs) in the toxic dinoflagellate *Alexandrium tamarense.* J Photochem Photobiol B 84:204–212

Carreto JI, Carignan MO (2011) Mycosporine-like amino acids: relevant secondary metabolites. Chemical and ecological aspects. Mar Drugs 9:387–446

Carreto JI, Carignan MO, Daleo G, Demarco SG (1990) Occurrence of mycosporine-like amino-acids in the red-tide dinoflagellate *Alexandrium excavatum*: UV-photoprotective compounds? J Plankton Res 12:909–921

Carreto JI, Carignan MO, Montoya NG (2001) Comparative studies on mycosporine-like amino acids, paralytic shellfish toxins and pigment profiles of the toxic dinoflagellates *Alexandrium tamarense*, *A. catenella* and *A. minutum.* Mar Ecol Prog Ser 223:49–60

Carreto JI, Carignan MO, Montoya NG (2005) A high-resolution reverse-phase liquid chromatography method for the analysis of mycosporine-like amino acids (MAAs) in marine organisms. Mar Biol 146:237–252

Clementson LA, Parslow JS, Turnbull AR, McKenzie DC, Rathbone CE (2001) Optical properties of waters in the Australasian sector of the Southern Ocean. J Geophys Res 106:31611–31625

Conde FR, Churio MS, Previtali CM (2007) Experimental study of excited-state properties and photostability of the mycosporine-like amino acid palythine in water solution. Photochem Photobiol Sci 6:669–674

Cullen JJ, Lesser MP (1991) Inhibition of photosynthesis by ultraviolet-radiation as a function of dose and dosage rate — results for a marine diatom. Mar Biol 111:183–190

Davidson AT, Bramich D, Marchant HJ, Mcminn A (1994) Effects of UV-B irradiation on growth and survival of Antarctic marine diatoms. Mar Biol 119:507–515

de Salas MF, Eriksen R, Davidson AT, Wright SW (2011) Protistan communities in the Australian sector of the sub-Antarctic Zone during SAZ-Sense. Deep-Sea Res II 58(Spec Issue):2135–2149

Doyle SA, Saros JE, Williamson CE (2005) Interactive effects of temperature and nutrient limitation on the response of alpine phytoplankton growth to ultraviolet radiation. Limnol Oceanogr 50:1362–1367

Evans C, Thomson PG, Davidson AT, Bowie AR, van den Enden R, Witte H, Brussaard CPD (2011) Potential climate change impacts on microbial distribution and carbon cycling in the Australian Southern Ocean. Deep-Sea Res II 58(Spec Issue):2150–2161

Garcia-Pichel F (1994) A model for self-shading in planktonic organisms and its implications for the usefulness of ultraviolet sunscreens. Limnol Oceanogr 39: 1704–1717

Gröniger A, Sinha RP, Klisch M, Hader DP (2000) Photoprotective compounds in cyanobacteria, phytoplankton and macroalgae — a database. J Photochem Photobiol B 58:115–122

Hannach G, Sigleo AC (1998) Photoinduction of UV-absorbing compounds in six species of marine phytoplankton. Mar Ecol Prog Ser 174:207–222

Helbling EW, Villafañe VE, Holm-Hansen O (1994) Effects of ultraviolet radiation on Antarctic marine phytoplankton photosynthesis with particular attention to the influence of mixing. In: Weiler CS, Penhale PA (eds) Ultraviolet radiation in Antarctica: measurements and biological effects. American Geophysical Union, Washington, DC, p 207–227

Helbling EW, Chalker BE, Dunlap WC, Holm-Hansen O, Villafañe VE (1996) Photoacclimation of Antarctic marine diatoms to solar ultraviolet radiation. J Exp Mar Biol Ecol 204:85–101

Hernando MP, Ferreyra GA (2005) The effects of UV radiation on photosynthesis in an Antarctic diatom (*Thalassiosira* sp.): Does vertical mixing matter? J Exp Mar Biol Ecol 325:35–45

Hernando M, Carreto JI, Carignan MO, Ferreyra GA, Gross C (2002) Effects of solar radiation on growth and mycosporine-like amino acids content in *Thalassiosira* sp., an Antarctic diatom. Polar Biol 25:12–20

Hernando M, Schloss I, Roy S, Ferreyra G (2006) Photoacclimation to long-term ultraviolet radiation exposure of natural sub-Antarctic phytoplankton communities: fixed surface incubations versus mixed mesocosms. Photochem Photobiol 82(Spec Issue):923–935

Hernando MP, Carreto JI, Carignan MO, Ferreyra GA (2012) Effect of vertical mixing on short-term mycosporine-like amino acid synthesis in the Antarctic diatom, *Thalasiossira* sp. Sci Mar 76:49–57

Holm-Hansen OL, Helbling EW (1993) Ultraviolet radiation and its effects on organisms in aquatic environments. In: Young CS, Björn LO, Moan J, Nultsch W (eds) Environmental UV photobiology. Plenum Press, New York, NY, p 379–425

Ingalls AE, Whitehead K, Bridoux MC (2010) Tinted windows: the presence of the UV absorbing compounds called mycosporine-like amino acids embedded in the frustules of marine diatoms. Geochim Cosmochim Acta 74:104–115

Jeffrey SW, Smith H, Vesk M, Groenewoud K (1997) The occurrence of UV-A and UV-B absorbing compounds in marine microalgae. Phycologia 36:43–44

Jeffrey SW, MacTavish HS, Dunlap WC, Vesk M, Groenewoud K (1999) Occurrence of UVA- and UVB-absorbing compounds in 152 species (206 strains) of marine microalgae. Mar Ecol Prog Ser 189:35–51

Karentz D, McEuen FS, Land MV, Dunlap WC (1991) Survey of mycosporine-like amino acid compounds in Antarctic marine organisms: potential protection from ultraviolet exposure. Mar Biol 108:157–166

Kelly L, Ullrich S (eds) (2006) UV effects on aquatic and coastal ecosystems. Photochem Photobiol 82(Spec Issue): 831–1131

Kitidis V, Tilstone GH, Smyth TJ, Torres R, Law CS (2011) Carbon monoxide emission from a Mauritanian upwelling filament. Mar Chem 127:123–133

Klisch M, Hader DP (2000) Mycosporine-like amino acids in the marine dinoflagellate *Gyrodinium dorsum*: induction by ultraviolet irradiation. J Photochem Photobiol B 55: 178–182

Laurion I, Roy S (2009) Growth and photoprotection in three dinoflagellates (including two strains of *Alexandrium tamarense*) and one diatom exposed to four weeks of natural and enhanced ultraviolet-B radiation. J Phycol 45: 16–33

Laurion I, Lami A, Sommaruga R (2002) Distribution of mycosporine-like amino acids and photoprotective carotenoids among freshwater phytoplankton assemblages. Aquat Microb Ecol 26:283–294

Laurion I, Blouin F, Roy S (2003) The quantitative filter technique for measuring phytoplankton absorption: interference by MAAs in the UV waveband. Limnol Oceanogr Methods 1:1–9

Laurion I, Blouin F, Roy S (2004) Packaging of mycosporine-like amino acids in dinoflagellates. Mar Ecol Prog Ser 279:297–303

Lesser MP, Cullen JJ, Neale PJ (1994) Carbon uptake in a marine diatom during acute exposure to ultraviolet-B radiation — relative importance of damage and repair. J Phycol 30:183–192

Litchman E, Neale PJ, Banaszak AT (2002) Increased sensitivity to ultraviolet radiation in nitrogen-limited dinoflagellates: photoprotection and repair. Limnol Oceanogr 47:86–94

Llewellyn CA, Harbour DS (2003) A temporal study of mycosporine-like amino acids in surface water phytoplankton from the English Channel and correlation with solar irradiation. J Mar Biol Assoc UK 83:1–9

Llewellyn CA, White DA, Martinez-Vincente V, Tarran G, Smyth TJ (2012) Distribution of mycosporine-like amino acids along a surface water meridional transect of the Atlantic. Microb Ecol 64:320–333

Marchant HJ, Davidson AT, Kelly GJ (1991) UV-B protecting compounds in the marine alga *Phaeocystis pouchetii* from Antarctica. Mar Biol 109:391–395

Marcoval MA, Villafañe VE, Helbling EW (2008) Combined effects of solar ultraviolet radiation and nutrients addition on growth, biomass and taxonomic composition of coastal marine phytoplankton communities of Patagonia. J Photochem Photobiol B 91:157–166

Metzl N, Tilbrook B, Poisson A (1999) The annual $fCO_2$ cycle and the air–sea $CO_2$ flux in the sub-Antarctic Ocean. Tellus B Chem Phys Meterol 51:849–861

Moisan TA, Mitchell BG (2001) UV absorption by mycosporine-like amino acids in *Phaeocystis antarctica* Karsten induced by photosynthetically available radiation. Mar Biol 138:217–227

Morrison JR, Nelson NB (2004) Seasonal cycle of phytoplankton UV absorption at the Bermuda Atlantic time-series study (BATS) site. Limnol Oceanogr 49: 215–224

Neale PJ, Banaszak AT, Jarriel CR (1998a) Ultraviolet sunscreens in *Gymnodinium sanguineum* (Dinophyceae): mycosporine-like amino acids protect against inhibition of photosynthesis. J Phycol 34:928–938

Neale PJ, Cullen JJ, Davis RF (1998b) Inhibition of marine photosynthesis by ultraviolet radiation: variable sensitivity of phytoplankton in the Weddell-Scotia Confluence during the austral spring. Limnol Oceanogr 43:433–448

Neale PJ, Davis RF, Cullen JJ (1998c) Interactive effects of ozone depletion and vertical mixing on photosynthesis of Antarctic phytoplankton. Nature 392:585–589

Norman L, Thomas DN, Stedmon CA, Granskog MA and others (2011) The characteristics of dissolved organic matter (DOM) and chromophoric dissolved organic matter (CDOM) in Antarctic sea ice. Deep-Sea Res II 58(Spec Issue):1075–1091

Pearce I, Davidson AT, Thomson PG, Wright S, van den Enden R (2011) Marine microbial ecology in the sub Antarctic Zone: rates of bacterial and phytoplankton growth and grazing by heterotrophic protists. Deep-Sea Res II 58(Spec Issue):2248–2259

Piazena H, Perez-Rodrigues E, Hader DP, Lopez-Figueroa F (2002) Penetration of solar radiation into the water column of the central subtropical Atlantic Ocean — optical properties and possible biological consequences. Deep-Sea Res II 49:3513–3528

Portwich A, Garcia-Pichel F (2003) Biosynthetic pathway of mycosporines (mycosporine-like amino acids) in the cyanobacterium *Chlorogloeopsis* sp. strain PCC 6912. Phycologia 42:384–392

Rastogi RP, Singh SP, Haeder DP, Sinha RP (2010) Mycosporine-like amino acids profile and their activity under PAR and UVR in a hot-spring cyanobacterium *Scytonema* sp. HKAR-3. Aust J Bot 58:286–293

Riegger L, Robinson D (1997) Photoinduction of UV-absorbing compounds in Antarctic diatoms and *Phaeocystis antarctica*. Mar Ecol Prog Ser 160:13–25

Riemer U, Lamare MD, Peake BM (2007) Temporal concentrations of sunscreen compounds (mycosporine-like amino acids) in phytoplankton and in the New Zealand krill, *Nyctiphanes australis* G.O. Sars. J Plankton Res 29: 1077–1086

Shick JM (2004) The continuity and intensity of ultraviolet irradiation affect the kinetics of biosynthesis, accumulation, and conversion of mycosporine-like amino acids (MAAs) in the coral *Stylophora pistillata*. Limnol Oceanogr 49:442–458

Shick JM, Dunlap WC (2002) Mycosporine-like amino acids and related gadusols: biosynthesis, accumulation, and UV-protective functions in aquatic organisms. Annu Rev Physiol 64:223–262

Sinha RP, Hader DP (2008) UV protectants in cyanobacteria. Plant Sci 174:278–289

Sinha RP, Singh SP, Hader DP (2007) Database on mycosporines and mycosporine-like amino acids (MAAs) in fungi, cyanobacteria, macroalgae, phytoplankton and animals. J Photochem Photobiol B 89:29–35

Smith RC, Prezelin BB, Baker KS, Bidigare RR and others (1992) Ozone depletion: ultraviolet radiation and phytoplankton biology in Antarctic waters. Science 255: 952–959

Tartarotti B, Sommaruga R (2006) Seasonal and ontogenetic changes of mycosporine-like amino acids in planktonic organisms from an alpine lake. Limnol Oceanogr 51: 1530–1541

Tedetti M, Sempere R (2006) Penetration of ultraviolet radiation in the marine environment. A review. Photochem Photobiol 82:389–397

Tilstone GH, Airs RL, Martinez-Vicente V, Widdicombe C, Llewellyn C (2010) High concentrations of mycosporine-like amino acids and colored dissolved organic matter in the sea surface microlayer off the Iberian peninsula. Limnol Oceanogr 55:1835–1850

Trull T, Rintoul SR, Hadfield M, Abraham ER (2001) Circulation and seasonal evolution of polar waters south of Australia: implications for iron fertilization of the Southern Ocean. Deep-Sea Res II 48:2439–2466

van de Poll WH, Alderkamp AC, Janknegt PJ, Roggeveld J, Buma AGJ (2006) Photoacclimation modulates excessive photosynthetically active and ultraviolet radiation effects in a temperate and an Antarctic marine diatom. Limnol Oceanogr 51:1239–1248

Van Heukelem L, Thomas C (2001) Computer assisted high-performance liquid chromatography method development with applications to the isolation and analysis of phytoplankton pigments. J Chromatogr A 910:31–49

Vernet M, Whitehead K (1996) Release of ultraviolet-absorbing compounds by the red-tide dinoflagellate *Lingulodinium polyedra*. Mar Biol 127:35–44

Villafañe VE, Helbling EW, Holm-Hansen O, Chalker BE (1995) Acclimatization of Antarctic natural phytoplankton assemblages when exposed to solar ultraviolet radiation. J Plankton Res 17:2295–2306

Villafañe VE, Sundbäck K, Figueroa FL, Helbling EW (2003) Photosynthesis in the aquatic environment as affected by UVR. In: Helbling EW, Zagarese HE (eds) UV effects in aquatic organisms and ecosystems. Royal Society of Chemistry, Cambridge, p 357–398

Weatherhead EC, Andersen SB (2006) The search for signs of recovery of the ozone layer. Nature 441:39–45

Whitehead K, Hedges JI (2005) Photodegradation and photosensitization of mycosporine-like amino acids. J Photochem Photobiol B 80:115–121

Whitehead K, Vernet M (2000) Influence of mycosporine-like amino acids (MAAs) on UV absorption by particulate and dissolved organic matter in La Jolla Bay. Limnol Oceanogr 45:1788–1796

Whitehead K, Karentz D, Hedges JI (2001) Mycosporine-like amino acids (MAAs) in phytoplankton, a herbivorous pteropod (*Limacina helicina*), and its pteropod predator (*Clione antarctica*) in McMurdo Bay, Antarctica. Mar Biol 139:1013–1019

Wright SW, van den Enden RL, Pearce I, Davidson AT, Scott FJ, Westwood KJ (2010) Phytoplankton community structure and stocks in the Southern Ocean (30–80° E). Deep-Sea Res II 57(Spec Issue):758–778

Zepp RG, Callaghan TV, Erickson DJ (2003) Interactive effects of ozone depletion and climate change on biogeochemical cycles. Photochem Photobiol Sci 2:51–61

Zudaire L, Roy S (2001) Photoprotection and long-term acclimation to UV radiation in the marine diatom *Thalassiosira weissflogii*. J Photochem Photobiol B 62:26–34

*Editorial responsibility: Ronald Kiene, Mobile, Alabama, USA*

*Submitted: May 30, 2012; Accepted: August 20, 2013*
*Proofs received from author(s): November 15, 2013*